PN ACL-839
109573

FINAL REPORT

Covering Period: 11/95 - 12/00

Submitted to the Office of the Science Advisor
U.S. Agency for International Development

DEVELOPMENT OF A GEOGRAPHIC INFORMATION SYSTEM FOR ASSESSMENT OF SUITABLE AREAS FOR RUNOFF IRRIGATION

Principal Investigators: Dr. Gennady Carmi, Dr. Pedro Berliner, Dr. Arnon Karnieli
Grantee Institution: Jacob Blaustein Institute for Desert Research, Ben-Gurion University of the Negev

Collaborator: Dr. Lev Poberezshsky
Institution: Scientific-Research and Design-Survey Association "Vodproject"

Project Number: CA 14-019

Grant Number:

A.I.D. Grant Project Officer:

Table of contents

EXECUTIVE SUMMARY

In many developing countries, limited irrigation water prevents good agricultural soil from being cultivated, causing a poor supply of food and, potentially, starvation. Optimization of use of existing water resources may benefit these countries by helping to increase agricultural production. In many arid areas, where rain is not sufficient for crop production, runoff water can be successfully harvested and used for irrigation. In Israel and in other parts of the world runoff water is used to grow a variety of crops.

In regions like the experimental basin of Sanzar river in Uzbekistan the agricultural activity is seriously restricted by the small amount of river water. At the same time there are sufficient rain water resources during spring which can be harvested, stored in soil and used by plants during the dry period. By harvesting runoff water in the Sanzar river basin, farmers can increase the area used for agricultural production and/or increase the crop yield.

In the Sanzar river basin area most of the local population is employed in growing and processing grapes. Favorable climatic and soil conditions, high-quality vineyards and the long tradition of grape cultivation has made this crop the main sources of the region's income.

Within the framework of the project CA14-019 " Development of a Geographic Information System for Assessment of Suitable Areas for Runoff Irrigation" we carried out the water harvesting part of field trials in Uzbekistan. Two experimental sites were chosen initially. The first was situated in the main experimental region – the Sanzar river basin in the Bakhmal District of the Djizak region. On the recommendation of the Uzbekistan team, the additional site was established at the Parkent river basin. The need for the second site was because detailed long-term rainfall-runoff data was available for this site and it was assumed to be similar to the main experimental region. In order to prove the similarity of these two sites the runoff harvesting experiment had to be carried out at both sites. In 1996 the Uzbekistan team built eight runoff plots at the Sanzar river basin and three runoff plots at the Pankent river basin and the first year of the field experiment was

1997. During the year only total values of rainfall and runoff for each event were measured. These data were not sufficient for comparison and the Uzbekistan team was asked to measure the rainfall and runoff rates for each event. Due to safety reasons (the Uzbekistan team had the problems with the local people) the experiments at the additional site at the Parkent river basin were stopped. Not having enough material for analysis to prove the similarity of two sites, it was decided to abandon the historical data at the additional experimental site.

In 1998 the Uzbekistan team measured rainfall and runoff rate for 1 runoff plot. Soil parameters were not measured in the field so it was necessary to use parameters from literature for the region. In 1999 the Uzbekistan team measured rainfall and runoff rates for the separate watersheds in the experimental region.

Both the experimental and historical data were used for calibration of the rainfall-runoff model and further use for rainfall-runoff relationship forecasting. Calibration was done with experimental data for the small plot. The model was verified for the large watershed, and a series of numerical forecasting was made. All forecastings were done with the assumption that rainfall data obtained during field measurements for the large watershed are representative for the region.

The model was used to analyse the relationship between Runoff cofficient (RC)and the watershed area, represented by the parameter Characteristic Flow Length (CFL) .. The calibrated and verified model was run for different CFL values on the experimental watershed and different runoff coefficients were obtained. The expert estimation for RC for any watershed in the region may be derived from the given analysis. The analysis also includes the consideration of relationship of the amount of water to be harvested for different CFL.

No field trial was carried out for estimation of the effect the amount of irrigation water on the yield and therefore some of the parameters needed for the model were unavailable so that the model could not be tested. Moreover, no soil survey was carried out and, thus, soil data, an important input into this type of model, was scarce. Soil depth, change of physical characteristics with depth,

presence of stones and water retention curve were lacking and had to be estimated based on the general description of the area. No radiation data was available and rainfall, temperature and humidity were available only as decade averages. In light of these severe constraints it was decided to develop a simple model to predict actual yield. We based the model on conventional knowledge of the crop as available in the literature.

The model gives a tool for the assessment of suitable areas for runoff harvesting in the region. Given different rainfall scenarios, the decision maker may obtain the desired results for amount of water to be harvested and the expected grape yield for a specific watershed. The modeled grape yield, for a given area of watershed, gave surprising results. It was found that for soil profiles of different depths, the grape yield did not increase with larger contributing areas of runoff.

GENERAL INTRODUCTION

Intensive irrigation of crops in arid and semi-arid regions, while in the short term provide economic incentives, may ultimately cause water shortages, health problems, economic hardship and irreversible environmental damage. In Uzbekistan over the last 30 years the diversion of two large rivers for cotton cultivation have caused the Aral sea, what once was the world's fourth largest inland sea, to shrink to only about one-third of its 1960 volume and to less than half its 1960 geographical size. The desiccation and increase of salinization of the lake have lead to widespread salt and dust storms from the sea's dried bottom, wreaking havoc on the region's agriculture and ecosystems and on the population's health. Desertification has led to the large-scale loss of biodiversity, loss of arable land, changed climatic conditions both locally and globally, and depleted yields on the cultivated land.

Thus, it is of prime importance to find alternative irrigation techniques to sustain the population in the future. Non conventional irrigation techniques have not been use in central Asia, particularly not in Uzbekistan. The use of runoff rain water may provide one such alternative. Large volumes of runoff water, which would otherwise be lost to evaporation and to infiltration, can be harvested and used for irrigating crops in arid and semi-arid regions. Under certain conditions, water harvesting (i.e. the use of surface runoff for agricultural production) can form a viable complement to irrigated agriculture.

The success or failure of rainwater harvesting depends to a great extent on the quantity of water that can be harvested from an area under given climatic conditions. The threshold retention of a catchment is the quantity of precipitation required to initiate runoff. It depends on various components such as surface storage, rainfall intensity, and infiltration capacity. The runoff efficiency, or runoff coefficient, of a watershed is the ratio of runoff volume to rainfall volume.

It is well known that because of reduced infiltration losses, the percentage of runoff increases with a decrease in watershed size (Amerman and McGuinnes, 1968). Small catchments (1-5

hectares) can produce runoff amounting to 10-15% of the annual rainfall. For microcatchment (10-500 sq.m), this can be even higher.

Site location and description

The landscape of Uzbekistan, (area - 447,000 square kilometers; population - 26.5 million), consists primarily of deserts, mountains and unploughed fields. Approximately 9% of the land is arable with agriculture representing 43% (26%) of the countries GNP. Cotton accounts for 35% of the total agricultural production, with 60-70% of it exported.

Water resources, which are unevenly distributed, are in short supply in most of Uzbekistan. The vast plains that occupy two-thirds of Uzbekistan territory have little water, and there are few lakes. The two largest rivers feeding the Aral sea are the Amudarya and the Syrdarya, which originate in the mountains of Tadjikistan and Kyrgyzstan. These rivers form the two main river basins of Central Asia; they are used primarily for irrigation, and several artificial canals have been built to expand the supply of arable land in the Fergana Valley and elsewhere. The irrigated areas are constantly enlarged and currently stand at 4.3 million hectares which is 95 % of the agricultural land in Uzbekistan. Most of the country is arid, with average annual rainfall amounting to between 100 and 200 mm and occurring mostly in winter and spring.

The area chosen for research is situated in the Sanzar River Basin in Djizak province, in the so-called Sanzar-Nouratau depression between Turkestan and Mal'guzar mountain ridges. The absolute heights vary from 350 to 1500 m MSL. According to agroclimatic division of Uzbekistan the Sanzar River Basin belongs to Zaamin agroclimatic district.

The Sanzar river is part of the Sydarya basin. The Sanzar river ends in the irrigation fan of the Djizak town and does not actually reach the Sydayra. The area of the Sanzar basin spans 2500 km^2, with the length of the main part of the river being 106km. One of the main tributaries of the Sanzar river is the Bakhmazarsai river with watershed area of 12.1 km^2 and a flow of 0.39 m^3/s. The rainfall and runoff field measurements were made at the Bakhmazarsai basin. Between 1996 and1999 there was relatively low precipitation, with the average Sanzar river flow of 0.93 m^3/s which is 49% of average flow.

Soils

Sanzar basin is a wide, hilly plain that has a vast low depression with a slightly hilly relief. The general slope is in a north-west direction and is bisected by ephemeral streams. The soils are mainly brown and gray-brown mountain-forest soils; vegetation is characterized by mountain and semi-desert couch grass and sagebrush associations. The soils are typical and dark serozoms and are brown alkaline soils on loess and silt rock proluvium and undergo erosion. Exact characteristics of all soil types depend on elevation, relief and slope exposition.

Agriculture in the Sanzar basin

The area under research has good soil potential for agriculture, but because of water scarcity, agriculture is limited. The dissected relief makes cotton problematic in the Sanzar river basin. Grapes have been cultivated in this area since historical times. The irrigation requirements of grape crop is suitable with the natural hydrographs of the water streams. At present, there are 1167 hectares of grape crops. Thus, we chose grapes as a crop for the testing of runoff irrigation.

RESEARCH OBJECTIVE

The overall aim of this study was to evaluate the suitability of runoff irrigation techniques for grape cultivation in an a arid region. Specifically, our objectives were to:

1) Cultivate vineyards in experimental sites to assess the effect of runoff irigation on grape yield.
2) Monitor water quality.
3) Caibrate a rainfall-runoff model through harvesting runoff water in designated plots.
4) Identify potential runoff irrigation locations through a development of a Geographic Information System of the region.

RAINFALL-RUNOFF MODEL

INTRODUCTION

The hydrology of arid and semiarid watersheds is characterized by high intensity, limited area extent precipitation, limited soil moisture, high evaporation, large transmission losses, and low annual surface water yield (Renald, 1979). The intensity of rainfall may be more important than the total amount, although runoff tends to increase with the duration of the rain event. Most ephemeral channels discharge water only when a moderately heavy rain falls on the drainage basin. Because of high evaporation losses and sparse vegetation, the degree of slope exercises a stronger control on the amount of runoff in arid areas than in humid areas. On desert hill slopes, runoff is rapid and the length of overland flow before the channel entrance is small. As a result, a fine network of slope rills is formed, and these link up into a channel network incised to varying degrees, depending upon rock resistance. The surface water yield per unit area generally decreases with increasing watershed area. This phenomenon is a result of large transmission losses in the major channels of the drainage network that contain large volumes of coarse textured high porosity alluvium.

RAINFALL-RUNOFF MODELS

The quasi-linear, spatially distributed cell models are classified as a lumped parameter, quasi-linear storage model. The attractive features of lumped models are that they need a relatively small number of parameters and are generally simpler than more complex runoff simulation models. However they do not purport to simulate the physical processes operating on a watershed, the output of lumped parameter models may be less accurate than more complex models.

The kinematic wave watershed models are more comprehensive, non-linear models available for detailed runoff forecasting. KINEMAT model was selected over other models for use in this project because of its arid watershed perspective. In fact, the model was calibrated and verified with hydrologic data from Walnut Gulch Experimental Watershed, a densely gauged arid watershed

located in south-eastern Arizona as well as with data from the Avdat experimental runoff harvesting farm located in the Central Negev desert (Israel).

Although considered complex in its computations of the physical processes involved in the rainfall-runoff process, the kinematic wave model requires limited input information: field measured parameters that represent the geometry, roughness and infiltration properties of the actual watershed. The simplification of the complex topography to a combination of plane and channel sections, each with its own set of hydraulic properties and interconnected with other plane and channel sections greatly reduces the efforts to eliminate the real parameter distribution over the watershed.

METHODS

For a cultivated area that is irrigated by runoff, it is vital to ascertain the potential runoff to be generated in the watershed. The amount of runoff in a given site directly depends on the size of the collection area. Other parameters such as soil characteristics (hydraulic conductivity, porosity, rainfall intensity, rock content, roughness, capillary drive), relief, vegetation cover, etc. will also determine the amount of runoff produced.

When modeling the rainfall-runoff relationship for small carchment water harvesting (SCWH) several approaces can be used. The empirical model of Karnieli *et al.* (1988) provides a design tool for the SCWH system in the Negev desert of Israel, and it incorporates the Partial Area Contribution Concept (PAC). The PAC concept states that measurable runoff is provided only from part of a given watershed. Humbog (1990), working in on a SCWH system in Mali, also came to the same conclusion regarding PAC. Dody *et al.* (1987) used parametric modeling for the entire watershed.

Vineyard irrigation experiment was an important component of our project. We intended to determine the water consumption enabling the maximum yields. The detailed description of the experiment was given in the proposal. At the fist meetings between Israeli and Uzbekistan team the

experiment conditions were specified and presented in the Annual report for the first year. According to the plan 16 experimental plots had to be set up within existing vineyard. Each plot had to had the area of 24x12m. Plots would be irrigated once a week and each plot will be irrigated by the following amount of water in four replicates: 1) without irrigation; 2) 25% of potential evapotranspiration; 3) 50% of potential evapotranspiration; 4) 100% of potential evapotranspiration. During the first year the experiment was not carried out. The Uzbekistan team explained by local difficulties. At our meetings with the Uzbekistan team we several times reduced our demands to the experiment to promote its carrying out. In spite of all our efforts experiment was not established. The Uzbekistan team stated it in the beginning of the third year of the project by the special letter to us. We reported about the situation in our annual report for 1998 and attached the letter of the Uzbekistan PI Dr. Pobereshsky. In order to overcome this serious limitation we decided to analyze available data of vineyard production and water consumption at Kolkhoz (collective farm) level for 1975-1997.

Runoff harvesting experiment.

As reported earlier two experimental sites were chosen initially. The first was situated in the main experimental region – the Sanzar river basin in the Bakhmal District of the Djizak region. On the recommendation of the Uzbekistan team the additional site was established at the Parkent river basin. The need for the second site was the fact that detailed long-term rainfall-runoff data was available for this site and it was assumed to be similar to the main experimental region. In order to prove the similarity of these two sites the runoff harvesting experiment had to be carried out at both sites. The first year of the field experiment was 1997 since the Uzbekistan team built in 1996 eight runoff plots at the Sanzar river basin and three runoff plots at the Pankent river basin. During the year only total values of rainfall and runoff for each event were measured. These data were not sufficient for comparison and the Uzbekistan team was asked to measure the rainfall and runoff rates for each event. Due to safety reasons (the Uzbekistan team had the problems with the local

people) the experiments at the additional site at the Parkent river basin were stopped. Not having enough material for analysis to prove the similarity of two sites, it was decided to give up the historical data at the additional experimental site.

In 1998 the Uzbekistan team measured rainfall and runoff rate for 1 runoff plot. According to the Uzbekistan team survey results the plot had the following features: area – 51 m^2, average slope – 0.34, saturated hydraulic conductivity – 17 mm/h, rock cover – 50%. It is necessary to note that one of the most important parameter for runoff calculation – saturated hydraulic conductivity – was not measured in the field but taken from literature for the region.

In 1999 the Uzbekistan team succeeded to measure rainfall and runoff rate for the separate watershed in the experimental region.

Runoff was measured using a calibrated pit and the water depth measurement inside the pit in equal intervals of time. For the large watershed the runoff was measured by the calibrated Thomson-Weir. The water level was measured manually at equal time intervals. Rainfalls were measured by the rainfall gauge with the surface of 500 cm^2.

During 1998 rainfall and runoff rate was measured for nine events for the runoff plot. After the careful analysis of the data the event of 4.04.98 was chosen for the model calibration. The rainfall rate for six events reached very high values, namely from 40 to 98 mm/h during tens of minutes. These very high values are not representative for the region and is likely to be a measurement error. Besides it the runoff measurements show relatively little amount of runoff during heavy events. The runoff measurements were done manually. In conditions of heavy rain the pit for water collection had to be overflowed. Most likely the errors in water volume measuring when pit was overflowing were sufficiently higher than for less heavy rains when there was not pit overflowing. So the model parameters were calibrated for the storm of 4.04.98 and verified for storms of 11.04 and 5.05.98.

Runoff simulation with KINEMAT rainfall-runoff model

KINEMAT (Woolhiser *et al.*, 1990) is a distributed, event oriented, physically based model describing the processes of surface runoff from watersheds. It is a distributed model because the watershed surface and channel network are represented by a cascade of planes and channels. Each plane may be described by its unique parameters, initial conditions, and precipitation inputs; and each channel, by unique parameters. It is an event-oriented model because it does not have components describing evapotranspiration and soil water movement between storms and therefore cannot maintain a hydrologic water balance between storms. Given initial soil moisture conditions, it calculates surface runoff for a single event. It is physically based because the mathematical models used to describe the components are based on such physical principles as conservation of mass and momentum. The geometry of the watershed is only an approximation of the real watershed.

Discussion of the model parameters

Rainfall input function

Rainfall was measured in one location with an automatic rainfall recorder situated in the village next to the experimental sites). Because of the relatively small areas of the experimental sites we assumed a homogeneous input function for the model calibration and forecasting.

Interception

As the rain falls on a vegetated surface, part of it remains on the foliage by surface tension forces, this is known as interception. Because the water does not reach the soil surface, it plays no part in infiltration. Thus, we subtracted the interception depth from the rainfall to calculate infiltration. In KINEMAT, the rainfall rate is reduced until the interception depth has been satisfied. If the total rain falling during the first time increment is greater than the interception, then the rainfall rate is reduced by the relation of the interception to the time step increment). For our

model, we used a an interception value valueof 1 mm that is typical for grass surfaces (Burgy and Pomeroy, 1958).

Depression storage capacity

This parameter is the average effective depth of water stored within the micro-depressions over the slopes. It directly affects the rate of overland flow that contributes to the stream channel after the rainstorm is terminated. Since the space distribution over the experimental area of this parameter was unclear, we used typical values for given surfaces in the model the.

Soil moisture and porosity

Soil moisture in the model is presented as relative to soil saturation, and is the ratio between volumetric soil water content and maximum water capacity. The maximum water content is measured as percent of porosity. Soil moisture monitoring was not carried out. The rain measurements were successful only for the part of the rain events and we could not develop the antecedent precipitation index (API) for the estimation of antecedent soil moisture. Nevertheless, in arid and semi-arid areas, antecedent soil moisture play a negligible role (Schreiber and Kincaid, 1967; Osborn and Renald 1973; Tauer and Humborg, 1992). The upper soil layers are unable to store moisture over extended periods due to the prevailing high temperatures. Girard (1975) suggests that the 750 mm isohyet is the lower limit for which antecedent soil moisture affects the rainfall-runoff relationship. Osborn and Renald (1973) concluded that the effect of antecedent soil moisture on runoff does not exceed 10% in the semi-arid southwestern USA. Albergel (1988), using rainfall simulation on soils with varying antecedent moisture conditions, obtained a similar result. For all of simulated events there was an antecedent rain. By the calibration process, we found the value of relative soil water content, provided the antecedent rain the day before, to be 80%. Porosity value used in the model was 46% which is typical for silt loam – loam soil types (Rawls, 1992).

Hydraulic conductivity

In the model, the same hydraulic conductivity values as for homogeneous soil were used. As sensitivity analysis of KINEMAT has shown, hydraulic conductivity is the most sensitive parameter of the model (Goodrich *et al.*, 1993). No field estimations of this parameter were obtained. The literature data collected by Uzbekistan team were initially used for the model calibration but these data found to be slightly higher to fit the simulation process. For the model calibration and runoff simulation, the value of saturated hydraulic conductivity was 13.5 mm/h. This value is typical for loam soils (Woolhiser *et al.*, 1990). Correspondingly, the value of capillary drive was chosen to be equal to 35 mm.

Infiltration and effective capillary drive

The infiltration expression of Smith and Parlange (1978) is used in the KINEMAT model

$$f = K \cdot \frac{\ell^{\frac{F}{B}}}{\ell^{\frac{F}{B}} - 1} \qquad (1)$$

where K is saturated hydraulic conductivity, F is infiltration depth, and B is defined as:

$$B = G \cdot (\theta_s - \theta_0) \qquad (2)$$

where G = effective net capillary drive (mm), θ_s = saturated water content, θ_0 = initial water content. B in equation (1) can be thought as the saturation deficit of the soil, which is the difference between the soil saturated capacity and its initial water content.

G is

$$G = \frac{1}{K_0} \int_{-\infty}^{0} K(\psi) d\psi \qquad (3),$$

where $K(\psi)$ = hydraulic conductivity function (mm/h), G = soil matric potential. G has units of length and can be thought of as a net or effective value of capillary head. G is conceptually a soil characteristic and does not incorporate the effect of initial water content, which is treated independently.

Equation (3) allows G to be derived from basic hydraulic characteristics of the soil relating unsaturated hydraulic conductivity to θ and ψ. It can also be considered a parameter to be determined from field experiments with infiltrometers. General estimates for G in this project were taken from Rawls et al. (1982) who compiled hydraulic data on a large number of soils over a range of textural classes.

For conditions of small amounts of infiltration depth, the expression $\ell^{\frac{F}{B}} - 1$ is close to zero, equation (1) becomes:

$$f=BK/F \qquad (4)$$

As already mentioned, the model which was designed for uniform homogeneous soil, assess the infiltration rate by means of expression (4) for $F/B < 0.1$ and by means of the expression (1) for $F/B \geq 0.1$.

Infiltration during recession

When the rain ceases or falls to a rate below the infiltration capacity, infiltration continues from the rain and from water still flowing on the soil surface until the water is locally depleted. Unlike rainfall, however, the supply of infiltrating water from flowing water cannot be assumed to be continuous over the surface. The kinematic treatment of the surface water flow does not require the assumption of "sheet" flow. On natural surfaces, flows are commonly confined to rivulets

according to the geometry of the microtopography. As a result, infiltration of surface water during recession is limited by the fraction of the soil surface exposed to the surface water.

KINEMAT provides a simple modification of infiltration during recession by describing the surface microtopography with a parameter RECS. This parameter represents, conceptually, the local maximum average depth of surface water flow for which the surface is essentially completely covered by the water. As average flowing water depth is reduced below this depth, the surface covered by the flowing water is assumed to decline in direct proportion to the depth. Thus when the local mean depth is half of RECS, the soil surface is assumed to be half covered by the flowing water. A very low value of RECS represents a relatively smooth soil surface, with little topographic variations, a large value of RECS represents a very rough surface, with flowing water confined to a small part of the surface. The ratio of water depth to RESC is used to reduce the net rate of loss of surface water by infiltration during recession conditions, as far as the surface water flow equations are concerned.

Overland flow

When the rainfall exceeds the infiltration capacity and overcomes surface tension, Hortonian overland flow begins. In KINEMAT model overland flow is approximated as a one-dimensional flow process in which the flux is proportional to some power of the storage per unit area. That is:

$$Q = \alpha \cdot h^m \qquad (5)$$

where Q is the discharge per unit width, h is the storage of water per unit area (or depth if the surface is plane), and α and m are parameters related to the slope, the slope roughness, and whether the flow is laminar or turbulent. Equation (5) is used in conjunction with the equation of continuity:

$$\partial h/\partial t + \partial Q/\partial x = q\,(x, t) \qquad (6)$$

where t is time, x is the spatial coordinate, and q (x, t) is the lateral inflow rate. If equation (5) is substituted into equation (6) we get

$$\partial h/\partial t + \alpha m h^{m-1} \partial h/\partial x = q(x,t) \qquad (7)$$

The kinematic wave equations are a simplification of the de Saint Venant equations and do not preserve all the properties of the more complex equations. It has been shown that the kinematic wave formulation is an excellent approximation for most overland flow conditions (Woolhiser and Liggett, 1967; Morris and Woolhiser, 1980).

For model application in this work the Manning hydraulic resistance law is used. In this option

$$\alpha = 1.49 \cdot \frac{S^{1/2}}{n} \text{ and } m = 5/3 \qquad (8)$$

where S is the slope, n is Manning's roughness coefficient, and English units are used.

Channel routing

Unsteady, free surface flow in channels is also represented by the kinematic approximation to the equations of unsteady, gradually varied flow. Channel segment may receive uniformly distributed, but time-varying lateral inflow from planes on either or both sides of the channel, or from one or two channels at the upstream boundary, or from a plane at the upstream boundary. The dimensions of planes are chosen to completely cover the watershed, so that rainfall on the channel is not directly considered. The continuity equation for a channel with lateral inflow is

$$\partial A/\partial t + \partial Q/\partial x = q_c(x, t) \qquad (9)$$

where A is the cross-sectional area, Q is the channel discharge, and q_c (x, t) is the net lateral inflow per unit length of channel. Under the kinematic assumption, Q can be expressed as a unique function of A and equation (9) can be rewritten as

$$\partial A/\partial t + (dQ/dA)(\partial Q/\partial x) = q_c (x,t) \qquad (10)$$

The kinematic assumption is embodied in the relationship between channel discharge and cross-sectional area.

$$Q = \alpha R^{m-1} A \qquad (11)$$

where R is the hydraulic radius. For Manning law that was used in the calculations, the equation (8) was used.

Description of the model variables used in the project

CHAR LENGTH – characteristic length (longest cascade of planes or longest single channel, whichever is greatest);

ENGLISH – if nonzero, English units;

METRIC – if nonzero, metric units;

ID NO – element identification number;

TYPE – denotes type of element; 1 = overland flow plane;

2 = trapezoidal open channel;

3 = circular pipe;

4 = detention pond;

5 = known inflow ("inject");

NU1 – ID number of an element contributing to the upper boundary of the current element;

NU2 - ID number of a second element contributing to the upper boundary of the current element;

NU3 - ID number of a third element contributing to the upper boundary of the current element;

NL1 - ID number of a plane contributing laterally to the current channel or pond;

NL2 - ID number of a second plane contributing laterally to the current channel or pond;

LENGTH – length of plane or channel;

WID/DIA – width of plane, bottom width of channel;

SLOPE – element slope in direction of flow;

BANK 1,2 – open channel side slopes;

MANNING – Manning's roughness coefficient "n";

INTER – interception depth;

COVER – fraction of area covered by intercepting vegetation;

KS – saturated hydraulic conductivity;

G – effective soil capillary drive;

POR – soil porosity;

SMAX – maximum relative soil saturation;

ROCK – relative soil volumetric rock content;

RECS – average micro-topographic relief of flow surface.

Model calibration results and discussion

The data of rainfall and runoff intensity measurements at the runoff plot were used for the model calibration. Runoff measurements were carried out as measurements of the water level in the calibrated pit over the regular time interval (from 5 to 20 minutes depending on the runoff intensity). Few field trial was carried out and therefore some of the parameters needed for the model could not be obtained. Soil physical characteristics had to be estimated based on the general description of the area and tested by the model calibration.

Data on the watershed calibration and verification are presented in table 1.

Event	Total rainfall, mm	Observed rainfall peak, mm/h	Observed total runoff, mm	Model total runoff, mm	Observed runoff peak, mm/h	Model runoff peak, mm/h	Observed runoff coefficient, %	Model runoff coefficient, %	Volume error, %
4.04.98	4.9	19.2	0.21	0.25	1.32	1.67	5	4.2	19
8.04.98	17.2	38.4	1.45	4.7	5.4	24.36	8	27	224
11.04.98	5.1	26.4	0.45	0.48	3.48	3.29	9	10	7
15.04.98	34.5	93.6	6.23	22.12	22.8	79.91	18	66	255
16.04.98	19.9	58.8	2.87	9.81	12.36	45.34	14	50	242
19.04.98	27.5	58.8	5.54	16.24	14.52	45.55	20	60	193
21.04.98	47.6	98.4	10.55	33.16	34.8	79.94	22	70	214
5.05.98	7.9	33.6	0.46	0.87	2.4	7.7	6	11	89
15.05.98	38.4	96.0	6.7	25.88	27	82.91	17	67	286

Table 1. Rainfall and observed and modeled runoff.

As noted, before the model was calibrated on the event of 4.04.98 and verified on two additional events: 11.04.98 and 5.05.98. Calibrated and verified hydrographs, as well total runoff amount, were estimated by means of the efficiency criterion (R^2) and the volume error (VE). R^2 and VE are described by the following expressions (Harlin and Kung, 1992):

$$R^2 = 1 - \frac{\sum_{i=1}^{i} [Q_m(i) - Q_0(i)]^2}{\sum_{i=1}^{i} \left[Q_0(i) - \bar{Q}_0(i) \right]^2} \qquad (12)$$

$$VE = 100 \frac{|T_m - T_0|}{T_0} \qquad (13)$$

$\bar{Q}_0$ – Mean observed runoff

Q_0 – Observed runoff

Q_m – Model runoff

T_0 - Total observed runoff

T_m - Total modeled runoff

i - total number of time steps

Small plots - 1998

In table 1 the results of runoff modeling at the runoff plot and their matching with observed hydrographs are presented. For three events the observed and model hydrographs have a similar shape. An efficiency criterion was in the range 50-70%. Nevertheless the total runoff amount for two events is very close to observed values. The least error for the event of 11.04.98 was 7%.

The calibration process showed that the model correctly simulates the total amount of runoff, but less accurately the hydrograph shape. But it is possible that the cause of low efficiency criterion

for the event 4.04.98 was a high measurement error since for other events the model gave acceptable results.

Some error of runoff beginning for model hydrograph is connected with uncertainty of real rain beginning in observed data. Very big time steps for rainfall input is the course of poor rainfall and runoff hydrographs peak matching in some cases. The calibration process showed that the model correctly simulates the total amount of runoff, but less accurately the hydrograph shape. But it is possible that the cause of low efficiency criterion for the event 4.04.98 was a high measurement error since for other events the model gave acceptable results.

Rainfall Event 4.04.98

Figure 3 shows the observed rainfall and observed runoff and modeled runoff on 4.04.98. The runoff volume were measured every 5 minutes. The observed rainfall peak was 19.2 mm/h, runoff peak – 1.32 mm/h. The rainfall duration was 70 min and total amount of precipitation was 4.9 mm. The observed runoff coefficient for the event was 5%.

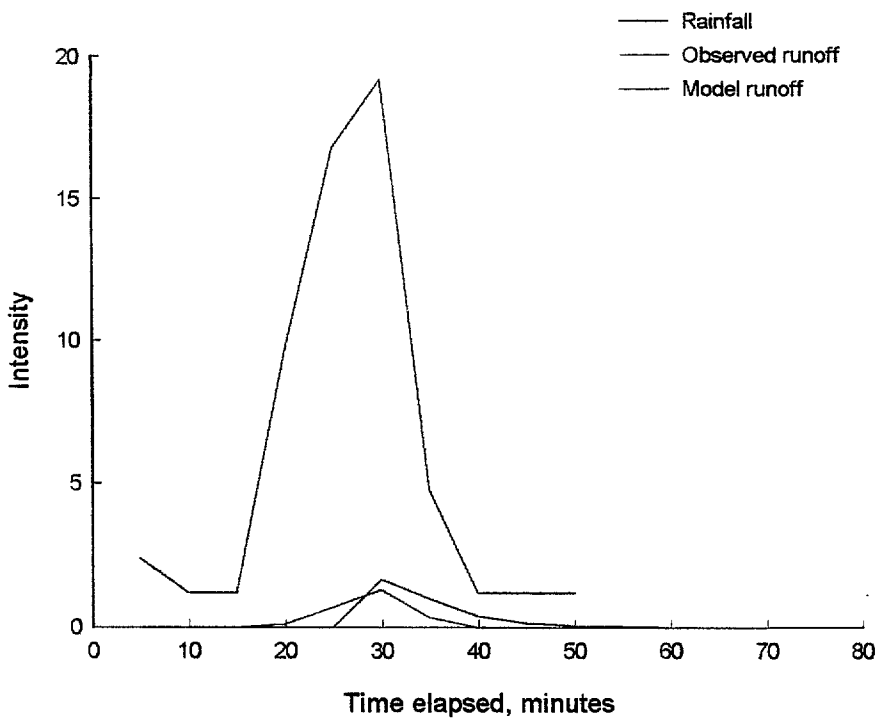

Figure 3. Rainfall and observed and model hydrographs on 4.4.98

Rainfall Event 11.04.98

Figure 4 shows the observed rainfall and observed runoff and modeled runoff on 11.04.98.The runoff volume were measured every 5 minutes. The observed rainfall peak was 19.2 mm/h, runoff peak – 1.32 mm/h. The rainfall duration was 70 min and total amount of precipitation was 4.9 mm. Observed runoff coefficient for the event was 5%.

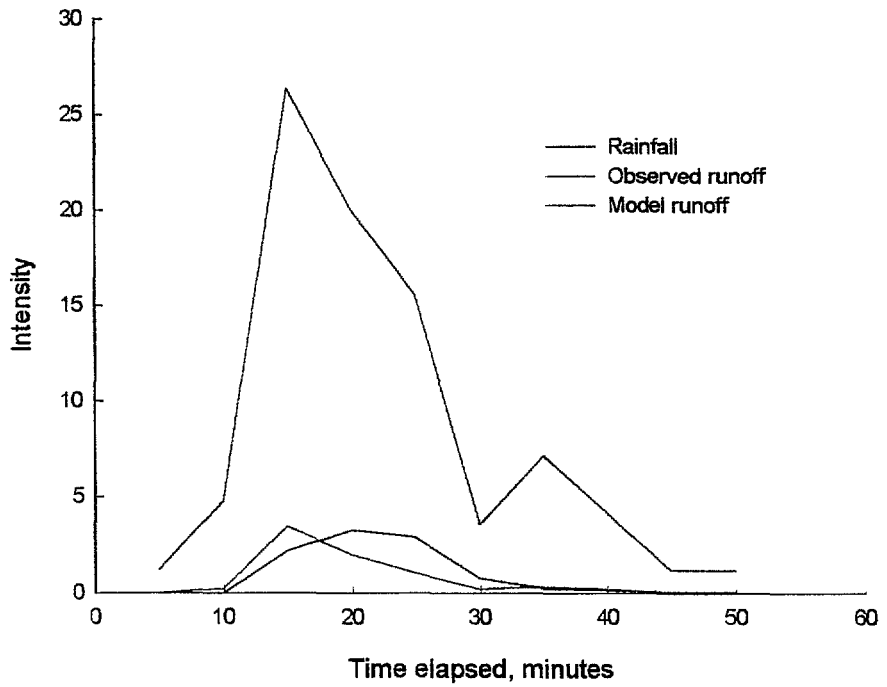

Figure 4. Rainfall and observed and model hydrographs on 11.4.98

Rainfall Event 5.05.98

Figure 5 shows the observed rainfall and observed runoff and modeled runoff on 5.05.98. The runoff volume were measured every 5 minutes. The rainfall peak was 33.6 mm/h, runoff peak – 2.4 mm/h. The rainfall duration was 55 minutes and total amount of precipitation was 7.9 mm. Total observed runoff was 0.46 mm. Observed runoff coefficient for the event was 6%.

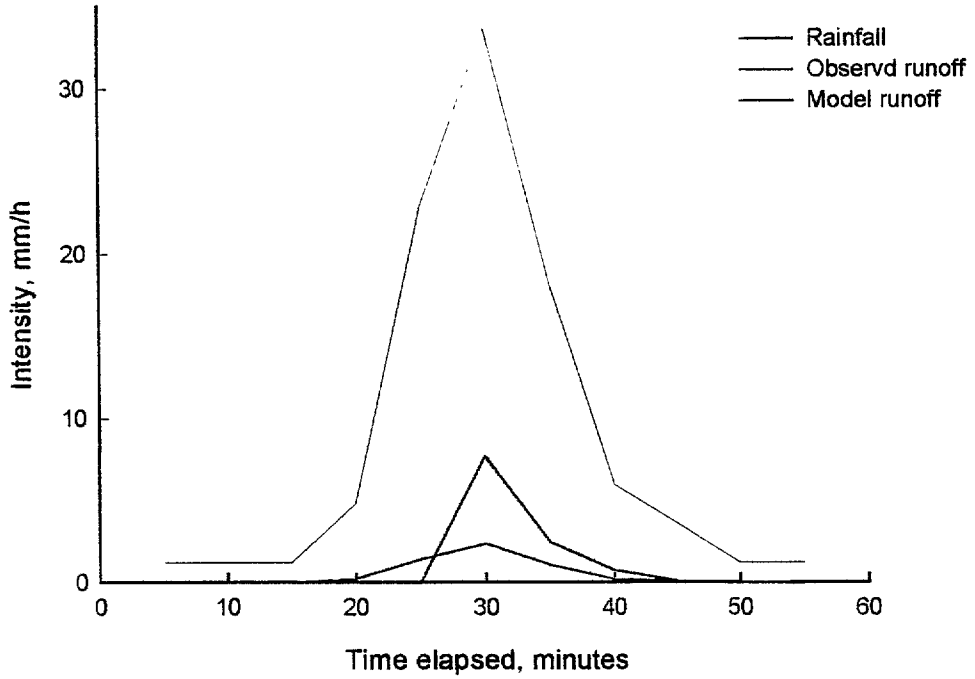

Figure 5. Rainfall and observed and model hydrographs on 5.5.98

Runoff forecasting for the large watershed

The aim of runoff forecasting the large watershed was to determine the relationship between the watershed area and the runoff coefficient. For this the rainfall and runoff rate measurements for the watershed with an area of ~ 0.3 sq. km were carried out.

There were four events for which rainfall and runoff rates were measured. The results of rainfall and runoff measurements were carefully checked and processed. Figure 6 shows the watershed and its model representation.

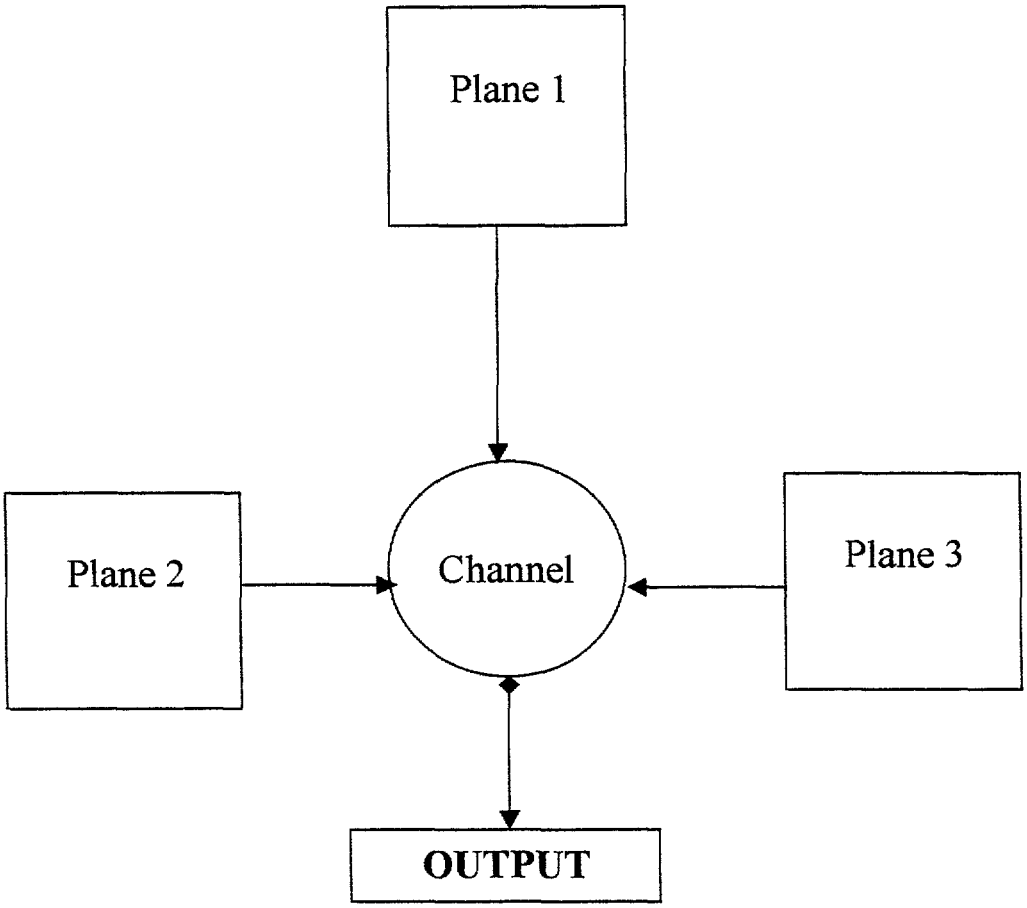

Figure 6. Symbolic representation of watershed model.

The experimental watershed is represented by three plane and one channel elements. The input for the model was the rainfall data for the specific event, and the output was the runoff hydrograph. The total runoff amount was compared with the observed runoff data. Figures 7-10 show the observed and modeled results.

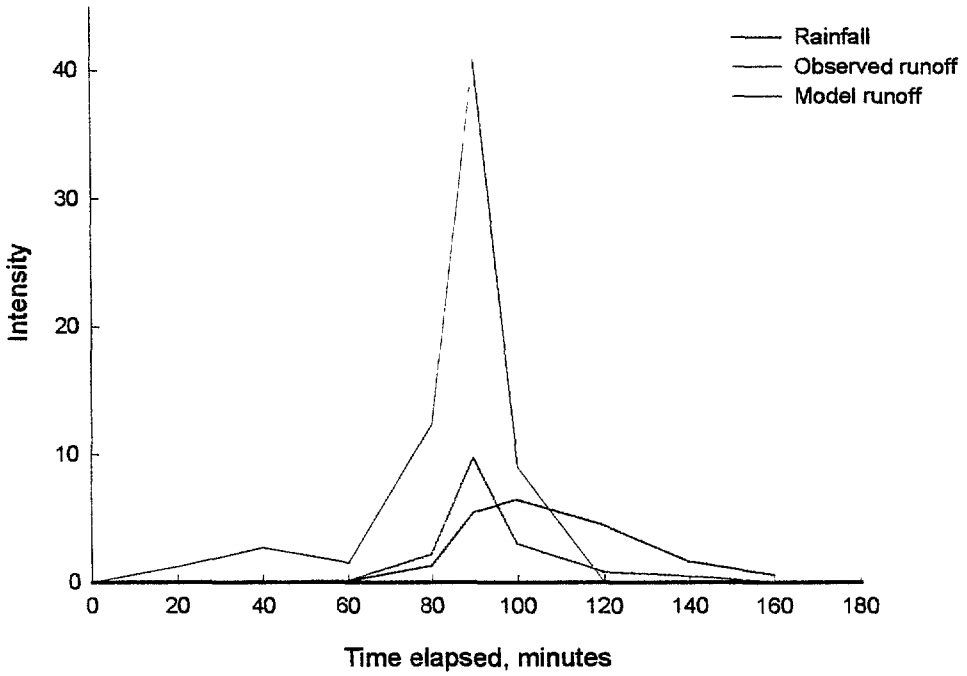

Figure 7. Rainfall and observed and model hydrographs on 25.3.99

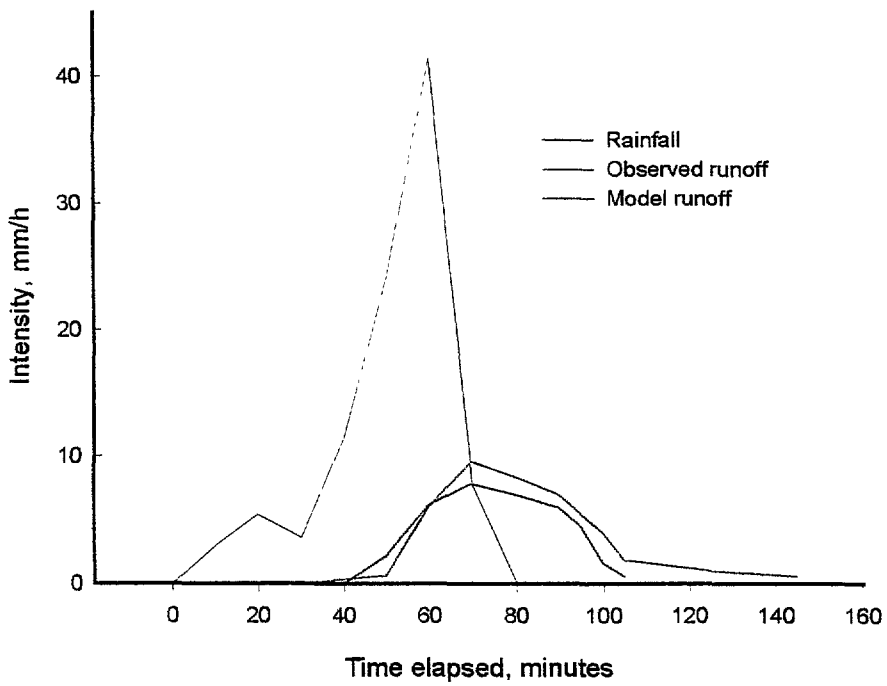

Figure 8. Rainfall and observed and model hydrographs on 10.4.99

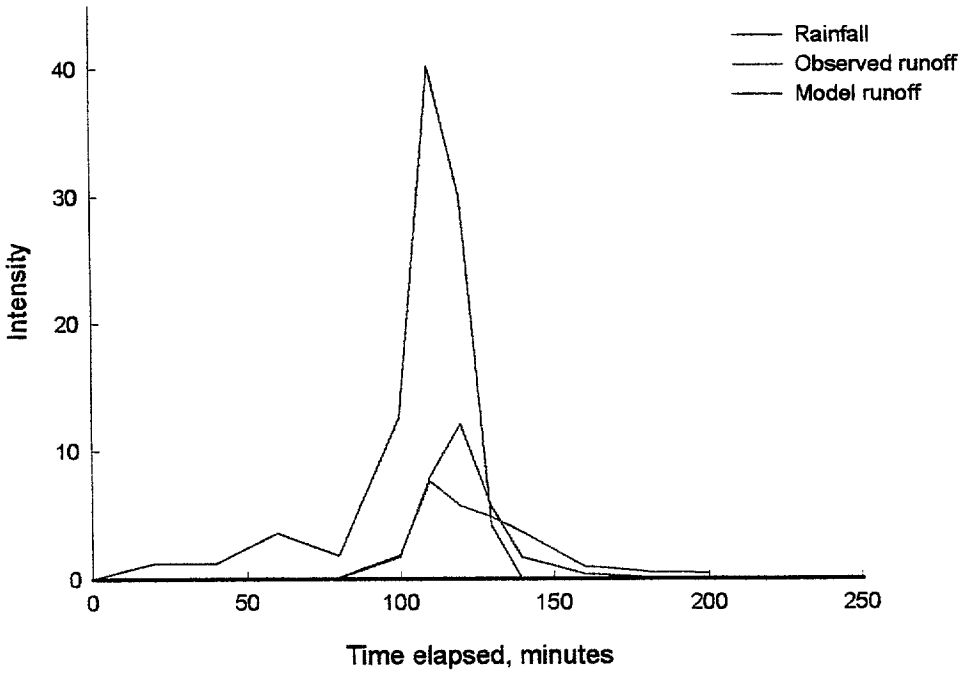

Figure 9. Rainfall and observed and model hydrographs on 29.5.99

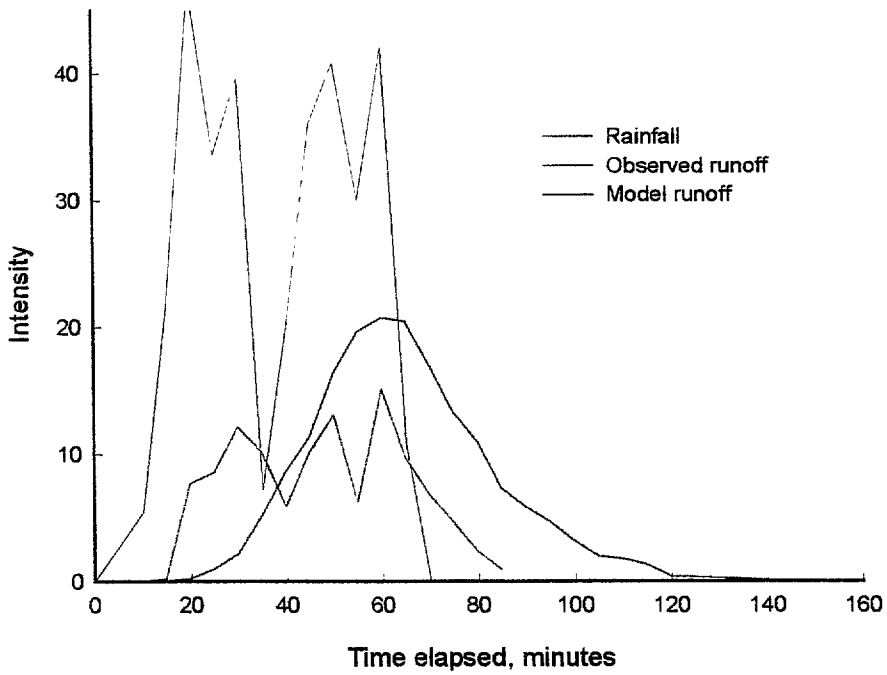

Figure 10. Rainfall and observed and model hydrographs on 23.6.99

Runoff coefficient - 1999

As was noted before, the runoff coefficient (RC) decreases with watershed size. The parameter "characteristic flow length" (CFL) is the average length of runoff flow. The calibrated model was run for different CFL on the experimental watershed and RC was obtained. Under the assumption that the experimental watershed and rainfall events are representative for the area, the expert estimation for RC for any watershed in the region may be derived from the equations given at the following figures.

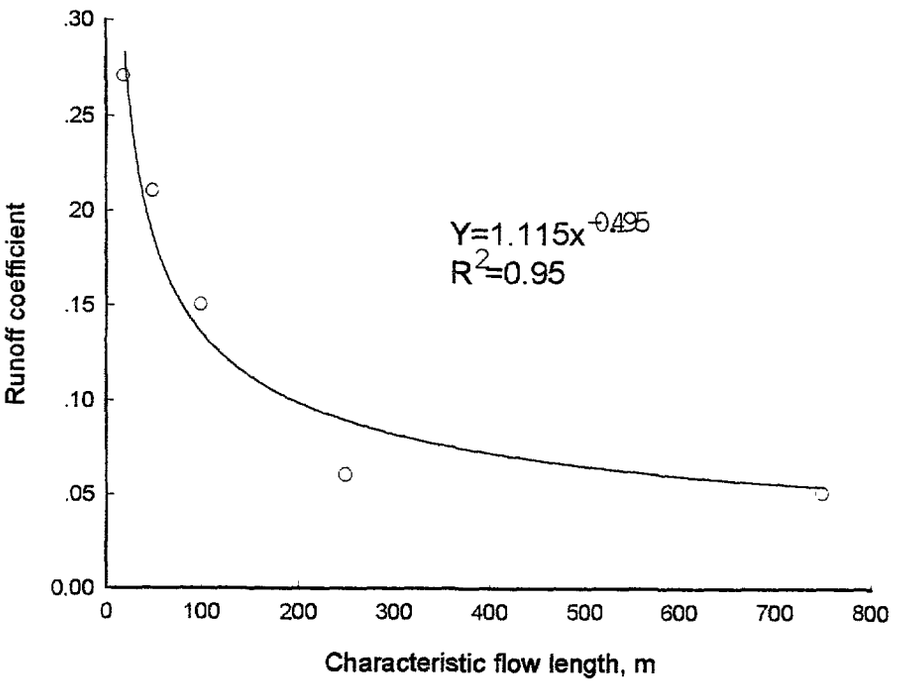

Figure 11. Runoff coefficient versus characteristic length on 25.3.99

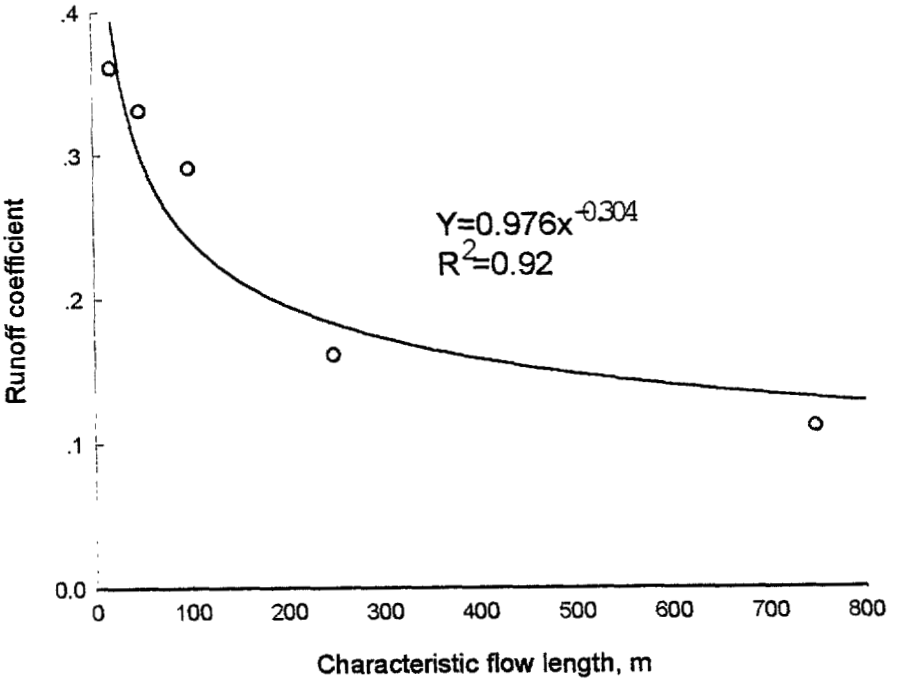

Figure 12. Runoff coefficient versus characteristic flow length on 10.4.99

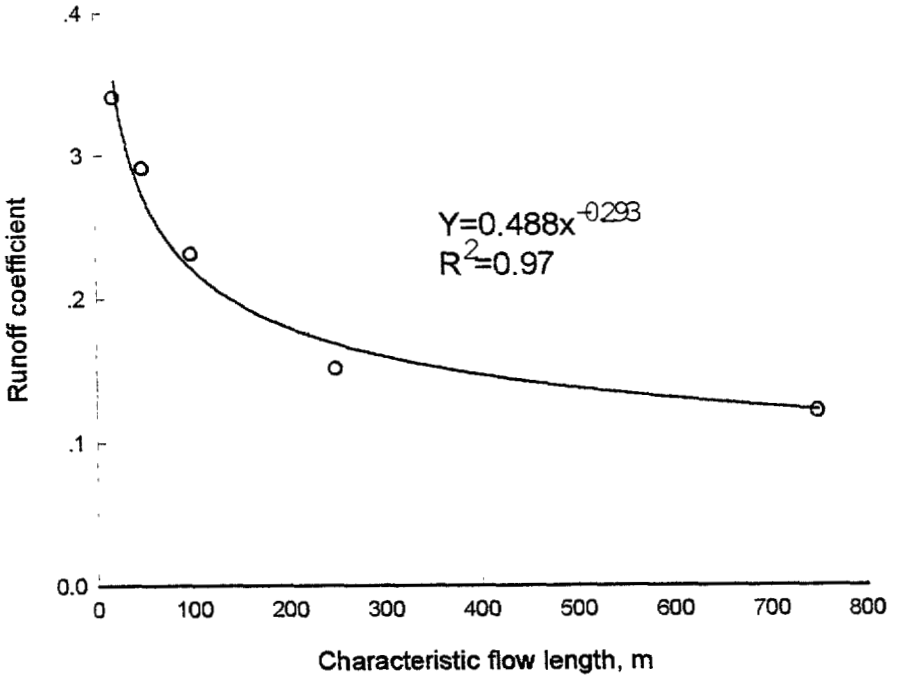

Figure 13. Runoff coefficient versus characteristic flow length on 29.5.99

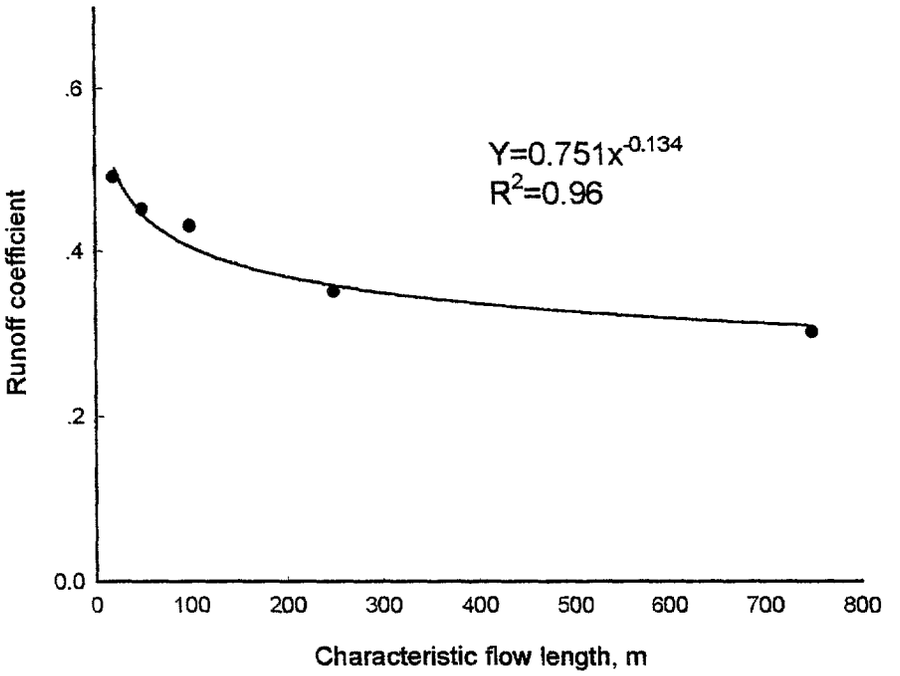

Figure 14. Runoff coefficient versus characteristic flow length on 23.6.99

Collected water – 1999

From the runoff coefficient it is possible to calculate the total amount of water collected and use these values in the model (see next section) to calculate grape yield. Figures 15 to 18 show the amount of water collected with the characteristic flow length of the watershed.

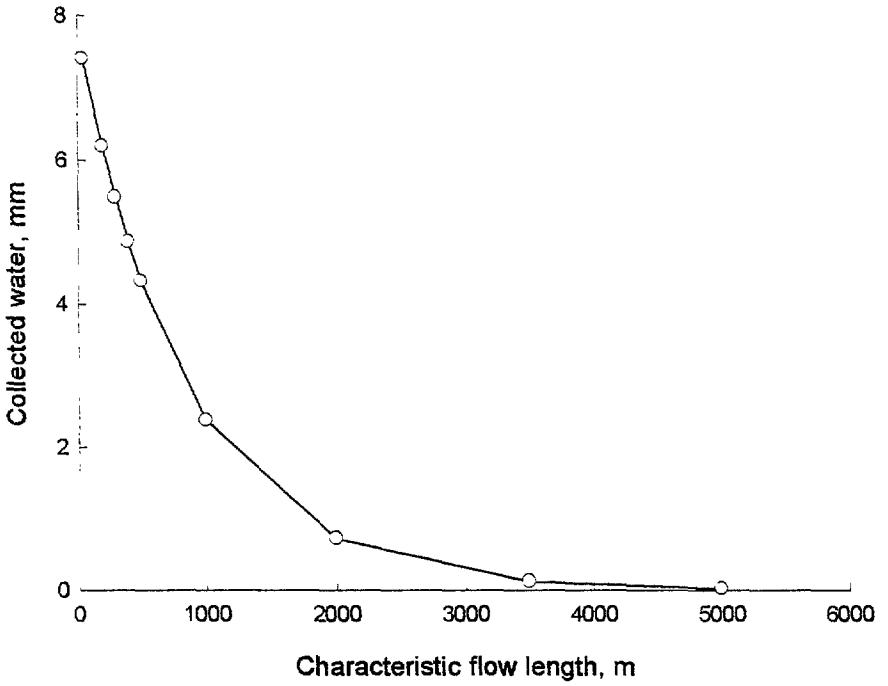

Figure 15. The effect of characteristic flow length on the collected water on 25.3.99.

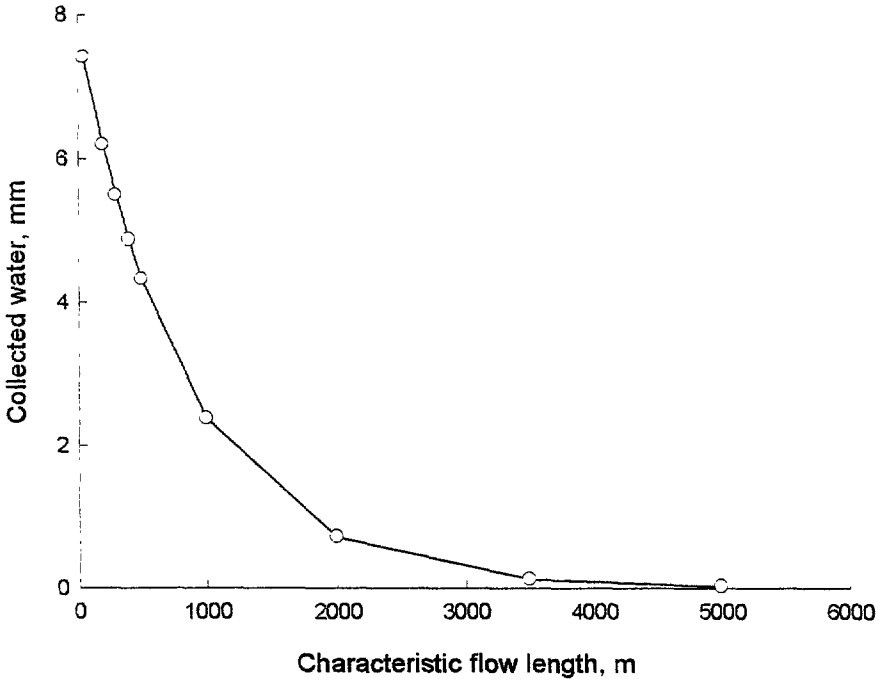

Figure 16. The effect of characteristic flow length on the collected water on 10.4.99

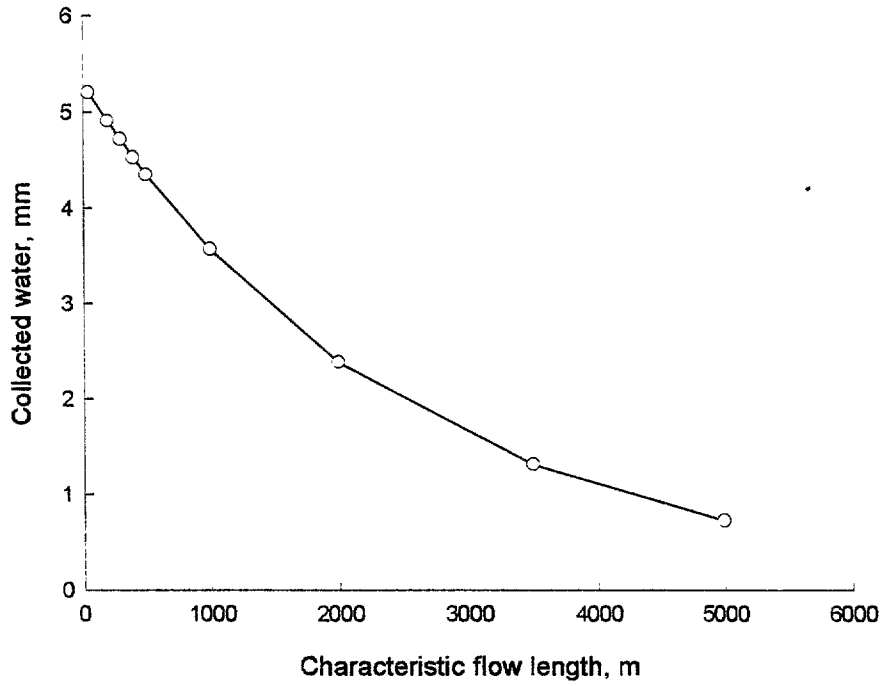

Figure 17. The effect of characteristic flow length on the collected water on 29.5.99

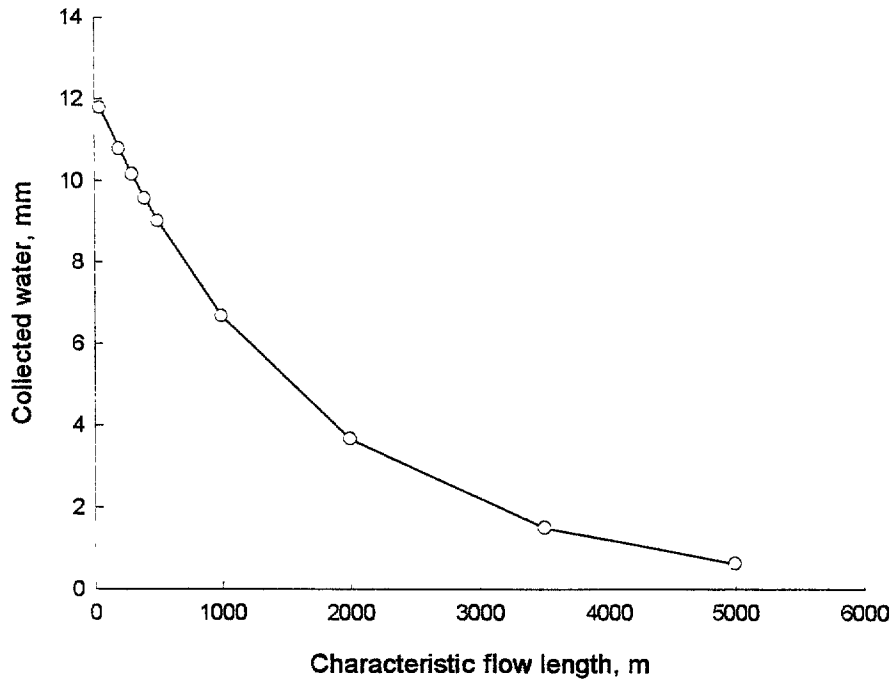

Figure 18. The effect of characteristic flow length on the collected water on 23.6.99

MODEL OF GRAPE YIELD PRODUCTION

INTRODUCTION

Runoff production depends, among others, on rainfall and has therefore the same variability. The runoff generated during a rainfall event can however be channeled to a dyke surrounded plot, and by proper selection of the ratio of contributing to receiving areas large volumes of water may be stored in the soil. The maximum amount of water worthwhile storing depends on the maximum rooting crop under consideration. Roots of grapes may reach great depths but under normal conditions the bulk of the water is absorbed to a maximum depth of 2 m. Arid and semi arid areas are characterized by low and erratic precipitation and by the fact that during large parts of the growing period of a crop water is a limiting factor. A classical way to circumvent this problem is by irrigating the crop during the dry period. In third world countries lack of infrastructure, capital and technical skills frequently make this approach impractical. Storing surplus of runoff water during the rainy season may be one of the alternative avenues to decrease water stress during the "dry" period, and attain therefore higher yields and decrease the year-to- year variability. We seek the solution by which we supply during most years the required volumes of water with the minimum of area devoted to the generation of runoff. Carrying out field trials in order to optimize the system is time consuming and site specific. The time span during which such trials are carried out has to be large due to the high interannual variability and the "site specificness" is due to the fact that small changes in slope, vegetation cover, orientation, etc. can yield significant differences in the runoff/rainfall ratio.

In the foregoing paragraph some of the problems associated with the optimal implementation of runoff irrigated crops have been pointed out. These limitations can be overcome by combining the use of remote sensing techniques to estimate the main parameters that affect runoff production coupled to a simple crop model that responds mainly to water stress and the availability of a relatively long record of climatic data. The strategy that we will use is to run the crop model for all

the possible runoff generating/runoff receiving combinations during the years for which data is available. The general trends of the response of the system can be evaluated.

MODEL

The model we need has to be relatively simple and respond to the main limiting factor, in our case, water. Hanks (1992) presented a modeling approach in which he showed predicted yield well during the linear response phase (to water) of the crop. The central idea of these types of models is that the relative yield (actual yield divided by the maximum yield attainable under the studied climatic conditions without suffering from water stress) is proportional to the relative transpiration (actual transpiration divided by the maximum transpiration attainable under the studied climatic conditions without suffering from water stress). The latter (a proxy for stress index) may be computed for each of the phonological phases or for the whole season. Doorenbos and Pruitt (1992) clearly point out that the there is no specific phonological effect in the case of grapes and we therefore developed a simple model for grape production based on Hank's approach without splitting the growth period into phonological periods.

PARAMETERS

Soil

We used the following soil parameters based on the gravimetric data supplied by the Uzbekistan team and by assuming a uniform bulk density of 1.35 $g \cdot cm^{-3}$:

Saturation: 0.55 $(m^3 \cdot m^{-3})$

Field capacity: 0.30 $(m^3 \cdot m^{-3})$

Wilting Point: 0.135 $(m^3 \cdot m^{-3})$

Climate data

Ten-day precipitation totals and ten-day averages of dry bulb temperature, sunshine hours, relative humidity and wind speed for 22 years (1975-1992) were available. In figure 1 the rainfall

distribution and the coefficients of variation ($CV=\sigma y/\overline{X_y}$) are presented. There was a marked variability that is particularly noticeable during the summer months. In figure 2 the annual course of ten-day sunshine hours is presented. The variability was not particularly high and decreased during the summer months. We found no correlation between rainfall and sunshine hours for any of the 12 months of the year. A tentative conclusion from this fact is that rainfall events are relatively short (probably less than a few days).

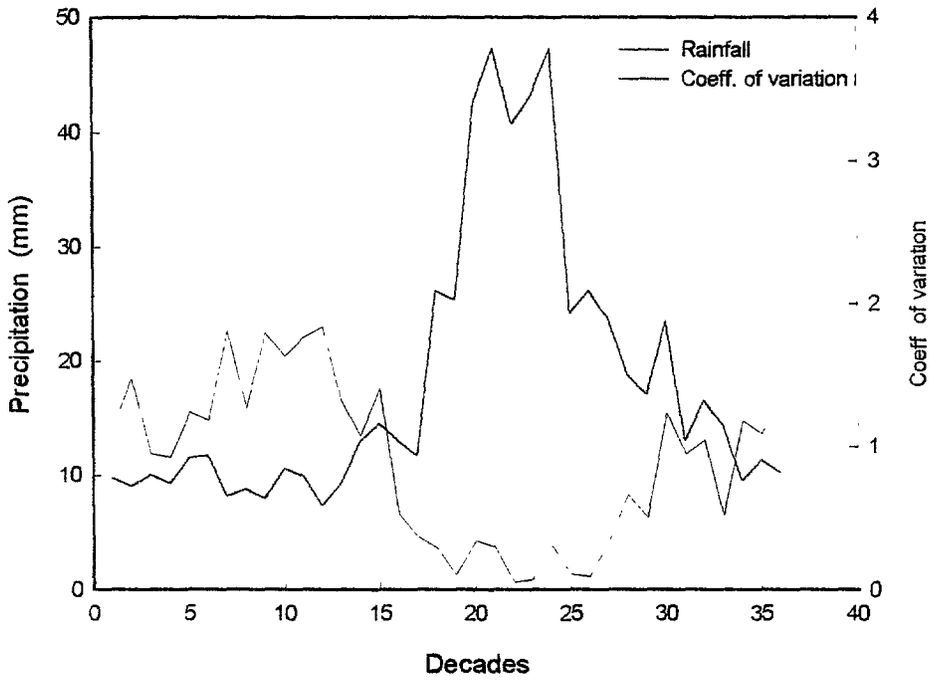

Figure 1. Rainfall average and coefficient of variation for 10-day periods.

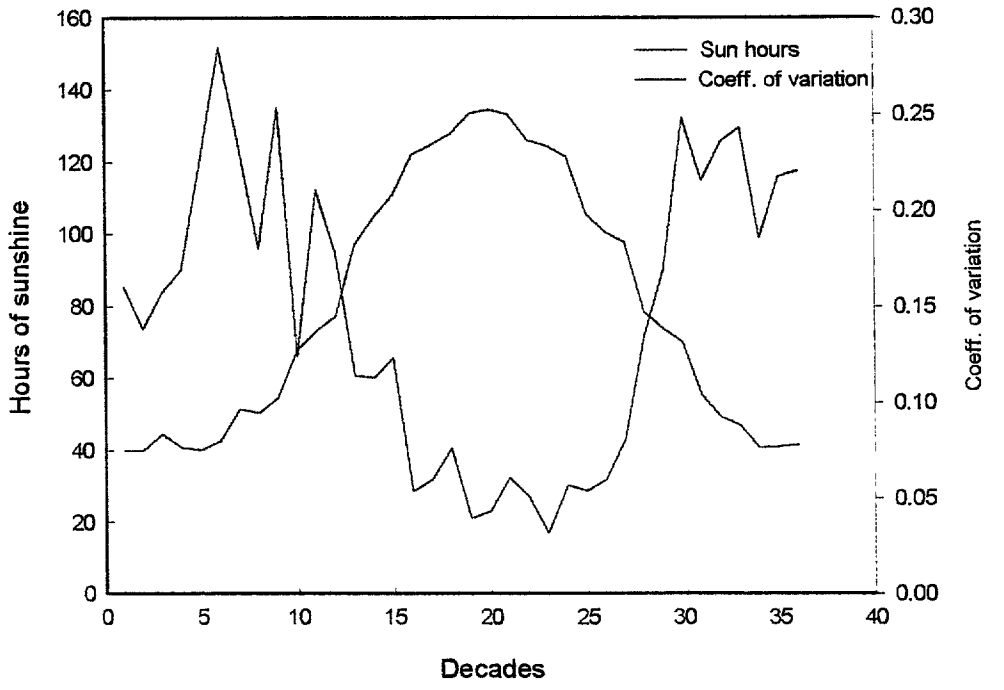

Figure 2. Sunshine average and coefficient of variation for 10-day periods.

Rainfall

We assumed that several rainfall events occurred during each of the decades. The number of rainy days (1-10), the actual serial day within each decade on which the event took place and the fraction of the decade's rainfall (0-1) corresponding to each of the selected days within a decade were all selected randomly.

Potential Evapotranspiration (PET)

PET for a decade was computed using:

$$PET = Q^* (s/(\gamma+s)) + (\gamma/(\gamma+s))\, Ku\, (e_a^* - e_a)$$

where

$Ku = 0.26\,(1 + 0.54\,U)$ [mm mb^{-1} day^{-1}]

U: wind speed at 2 m. height [m s^{-1}]

Q*: Net available energy [mm day^{-1}]

e_a: vapour pressure [mb]

e_a^* : vapour pressure at air temperature [mb]

s: slope of the saturated vapor pressure curve (ds/dT) [mb $^0C^{-1}$]

γ: psychometric constant {=0.66 mb $^0C^{-1}$)

Q*= NR-Gs

NR=Gr(1- Δ)+ L⇓ - L⇑

where

Gs: sensible heat flux in the soil [mm day^{-1}]

Gr: incoming short wave radiation [mm day^{-1}]

Δ: albedo

L⇓: incoming long wave radiation [mm day^{-1}]

L⇑: outgoing long wave radiation [mm day^{-1}]

and computed as follows:

$$L\Downarrow = \varepsilon a \sigma Ta4 = 1.24 (ea/Ta)1/7\sigma (Ta+273)4 \text{ [mm day}^{-1}\text{]}$$

$$L\Uparrow = \varepsilon s \sigma Ta4 \quad \text{[mm day}^{-1}\text{]}$$

σ: Boltzmann constant [W m^{-2} oK^{-4}]

$Gr = G_{EXT} (0.2+0.5*(N_S/M_{NS}))$ [mm day^{-1}]

N_S: number of sunshine hours

M_{NS}: maximum number of sunshine hours

G_{EXT}: Extraterrestrial incoming short wave radiation

Extraterrestrial incoming short wave radiation was computed for each decade using the formulae detailed in Sellers (1965) and the corresponding M_{NS} obtained from tables (Brutsaert, 1982). The annual course of computed PET is presented in figure 3.

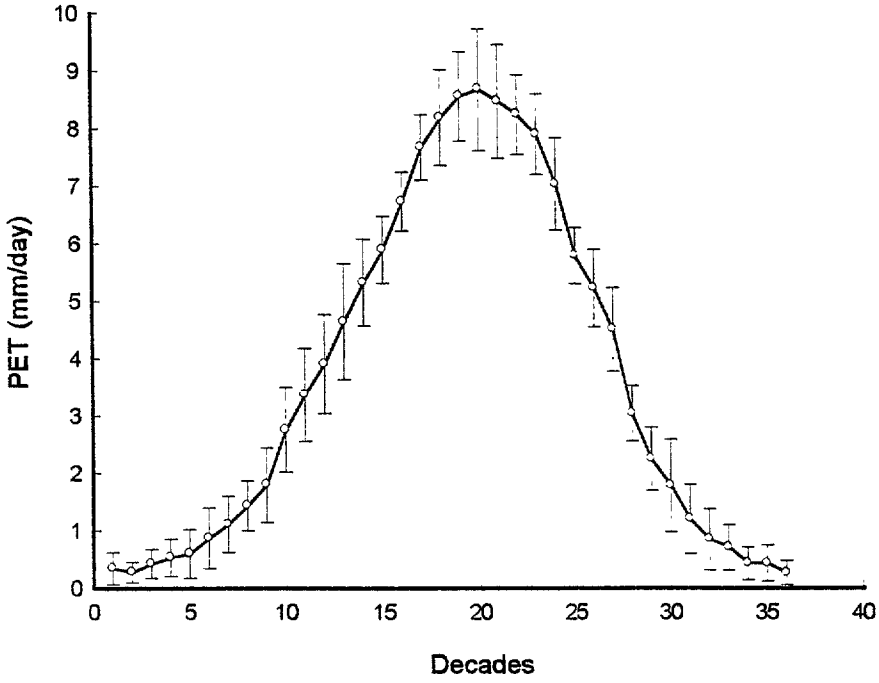

Figure 3. Average Potential evapotranspiration and standard deviation for 10 day periods

For decades without precipitation the computed PET was assumed to be constant. For decades with precipitation we arbitrarily assumed that on rainy days the PET was 1/3 of the computed decade value and the PET during the remaining days of the decade proportionally increased.

MODEL DESCRIPTION

The governing assumption of the model was that the ratio ET/PET is linearly related to water availability. For the simulation the soil profile was split into 0.5 m segments.

Evaporation during the period between harvest and bud bursting of the next season was assumed to depend only on the water content of the upper layer, and was computed as follows:

$$E = PET_d e^{\left[-a\left(1-\frac{SWC_d - WP}{SAT - WP}\right)\right]}$$

This parameterization describes an exponential decay in soil evaporation (E) with a decrease in the soil water content of the upper layer. At saturation E equals the PET. The value of "a" an

empirical parameter is to be determined from field observations which were not carried out. We selected a=10 based on previous experience with soils of similar texture.

During the growth period, i.e., between bud bursting and harvesting of the season, the ratio ET/PET varied linearly between two limits, which depend on the depth from which water is extracted and on water availability in the layer under consideration.

1. For the upper layer: $\underline{SWC_d \geq FC}$

$$\frac{ET}{PET} = Km\left(0.5 \cdot K_d\left[\frac{SWC_d - SAT}{FC - SAT}\right] + 0.5 \cdot K_d + \delta \sum_{d+1}^{n} K_d\right)$$

2. $\underline{FC} \leq \underline{SWCd} \leq \underline{WP}$

$$\frac{ET}{PET} = Km\left(K_d\left[\frac{SWC_d - WP}{FC - WP}\right] + \delta \sum_{d+1}^{n} K_d\right)$$

And for all remaining layers:

$$\frac{ET}{PET} = Km\left(K_d\left[\frac{SWC_d - WP}{SAT - WP}\right] + \delta \sum_{d+1}^{n} K_d\right)$$

where

d indicates the depth interval

δ=0 when d+1>n and δ=1 for all other cases

SWC_d: volumetric soil water content ($SAT \leq SWC_d \geq WP$)

WP : volumetric soil water content at wilting ($m^3\ m^{-3}$)

SAT: volumetric soil water content at saturation ($m^3\ m^{-3}$)

We define Etma as the maximum possible evapotranspiration possible for a given phonological stage assuming water is not a limiting factor and Km as the ratio ETma/PET . We defined Km for each month during the growing period

The values of Kd are as follows:

Soil depth (m)	K_1	K_2	K_3	K_4
0.5	1			
1	0.5	0.5		
1.5	0.33	0.33	0.33	
2	0.25	0.25	0.25	0.25

Water uptake proceeded sequentially from the uppermost to the deepest layer. Water was extracted from each layer until the lowest allowable water content (WP) was reached. Thereafter, water uptake took place from the underlying segment. Addition of water (from rainfall and/or runoff) followed the same sequence. The excess of water overflowed into the next underlying segment. The water not absorbed when the lowest segment has been filled up is defined as runoff loss. After the addition of water, uptake proceeded from the uppermost layer independently of the layer from which water had been withdrawn prior to the rainfall event.

The runoff coefficient was parameterized as a function of rainfall intensity and distance of overland flow was found using the results from the hydrological model. The following parameters were used:

$Eff=1.4049 * dist^{-.519}$ when total rainfall $\leq$ 16 mm

$Eff=1.2431 * dist^{-.3612}$ when 16 mm < total rainfall $\leq$ 19mm

$Eff=1.9373 * dist^{-.3162}$ when 19 mm < total rainfall $\leq$ 28mm

$Eff=0.7741 * dist^{-.1395}$ when total rainfall >28 mm

We assumed that the runoff water was conveyed to and spread over a soil strip 10 m wide (two rows of vines). We ran our model for a number of ratios of contributing to receiving areas (η): 0 (no runoff), 1, 2, 3, 4, 5, 7.5, 10, 15 and 20.

RESULTS AND DISCUSSION

As pointed out in the introduction no field trial was carried out and therefore some of the parameters needed for the model could not be obtained nor could the model be tested. Moreover, no soil survey was carried out and, thus, soil data, an important input into this type of model, was scarce. Soil depth, change of physical characteristics with depth, presence of stones and water retention curve were lacking and had to be estimated based on the general description of the area. No radiation data was available and rainfall, temperature and humidity were available only as decade averages. In light of these severe constraints it was decided to develop a simple model to predict actual yield. As Evapotranspiration (ET) is linearly related to consumptive water use when the latter is limiting (Doorenbos and Kassam,1992), we used ET as a proxy for yield. We based the model on conventional knowledge about the crop as available in the literature (Doorenbos and Kassam, 1992) irrigation of agricultural crops and additional articles.

The equivalent depth of runoff water added prior to bud burst during the studied period is presented in figure 4.

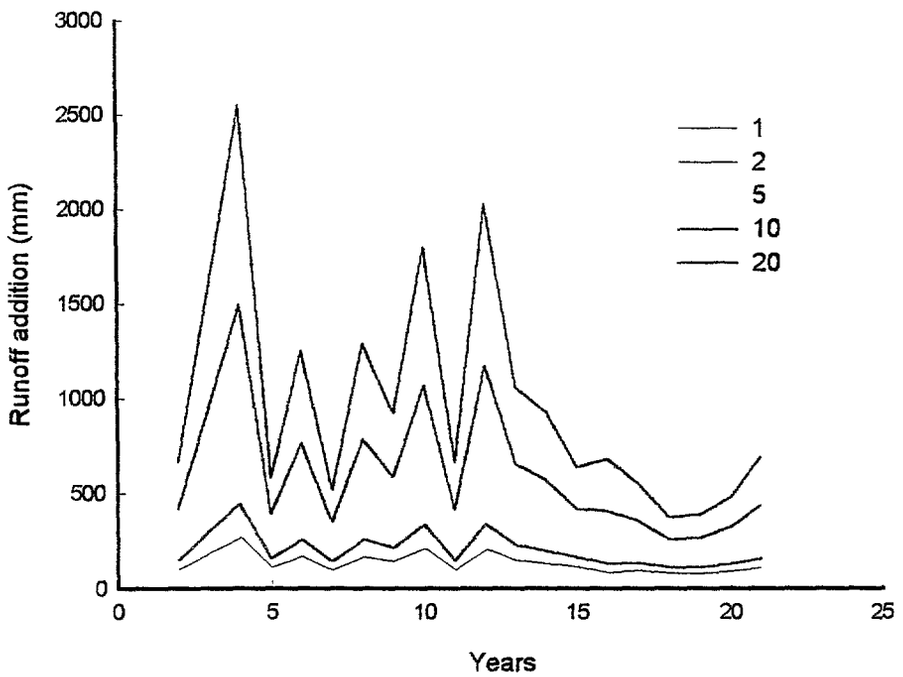

Figure 4. The equivalent depth of runoff water added prior to bud burst during the study period.

The effect of the contributing area is clear. The relatively small amounts added during the last five years are noteworthy. In figures 5 and 6 the equivalent depth of water lost for the shallowest and the deepest soil profile are presented. The fraction of water lost increased with an increase in the contributing area but was lower for the deeper soil profile.

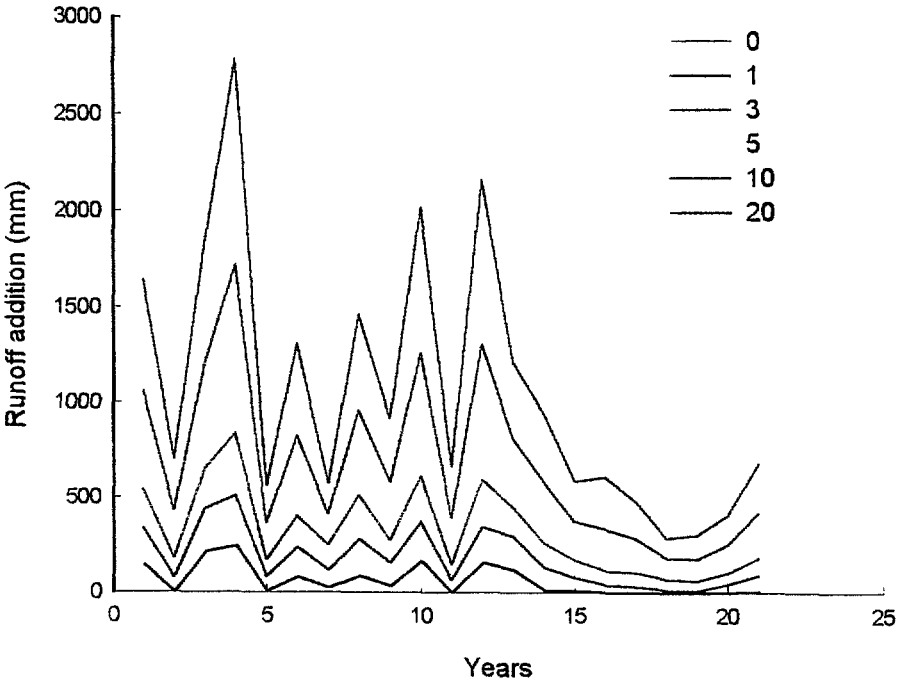

Figure 5. Equivalent depth of water lost for a soil profile with a depth of 0.5m during the study period for different watershed surfaces (η)

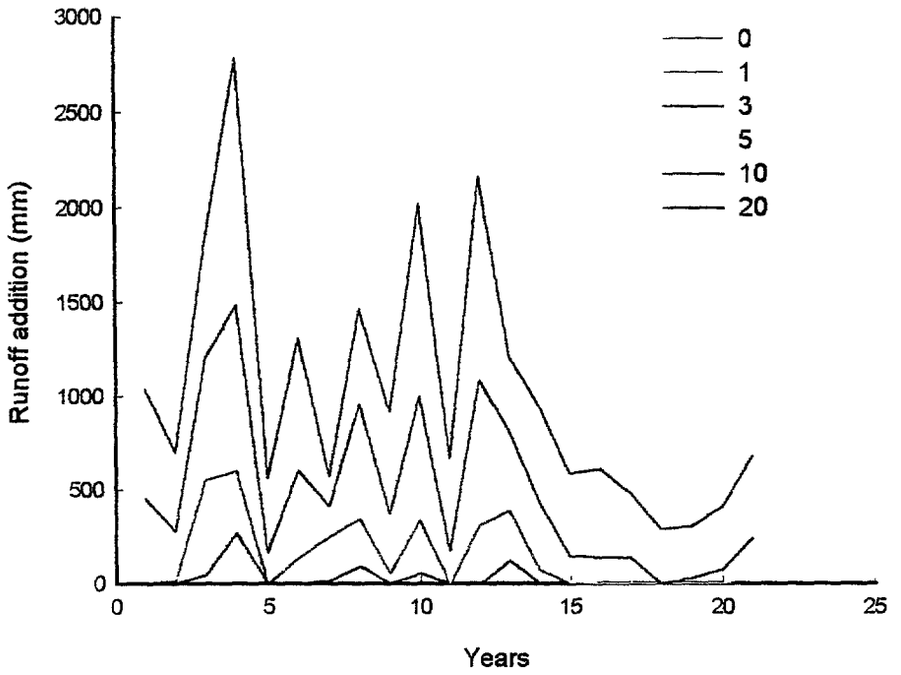

Figure 6. Equivalent depth of water for a soil profile with a depth of 2m during the study period for different watershed surfaces (η).

In figure 7 the equivalent depth of water added during the growing season is presented. The variability is proportional to the contributing area. For the smallest contributing area considered, the addition is small. In some years the precipitation during the summer months was extremely low.

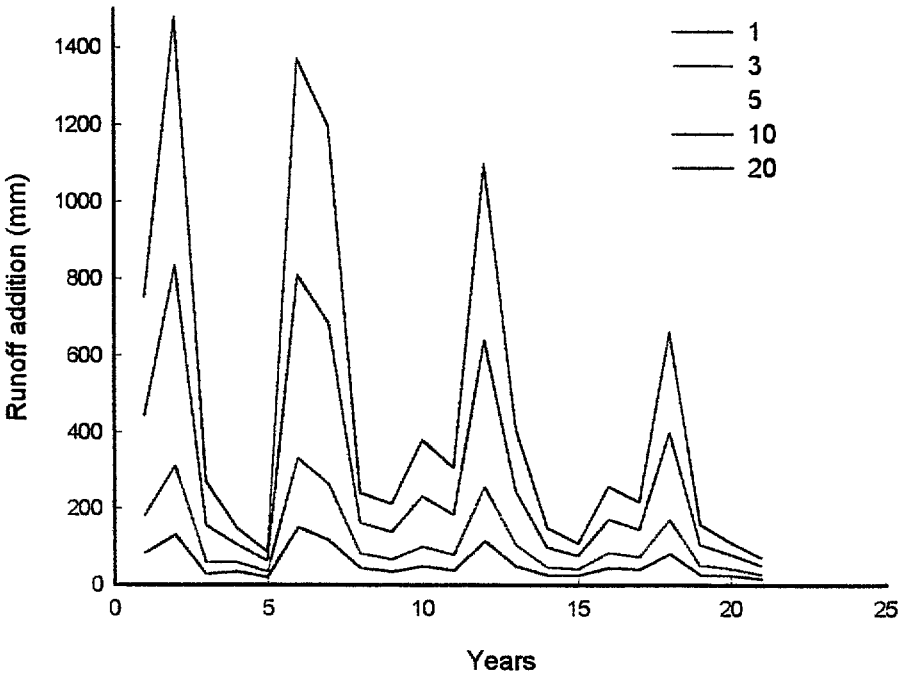

Figure 7. The equivalent depth of water added during the growing season for different watershed surfaces during the study period.

The ratio ET/ETma for the growth period (a proxy for yield) during the studied period is presented in figures 8 to11 for the four soil depths. The differences are small for the shallowest soil profile and the ratios are highest, as expected, for those years during which summer precipitation was high. Increase in soil depth resulted in an increase in the overall ET/ETma ratio for all contributing areas. The year-to-year fluctuations decreased with an increase in soil depth and are minimized for the 2 m deep soil profile when η, the ratio of the contributing area to the receiving area, is greater than 2. An increase in the contributing area did affect the evapotranspiration ratio and the water was lost as is evident in figures 5 and 6.

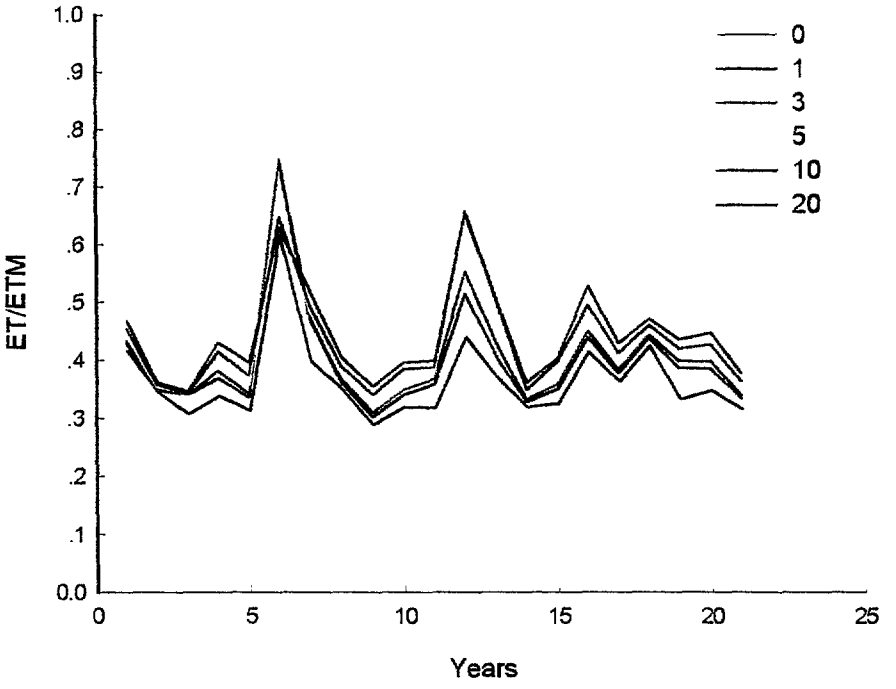

Figure 8. ET/ETma for a soil profile with a depth of 0.5m during the study period for different watershed surfaces (η).

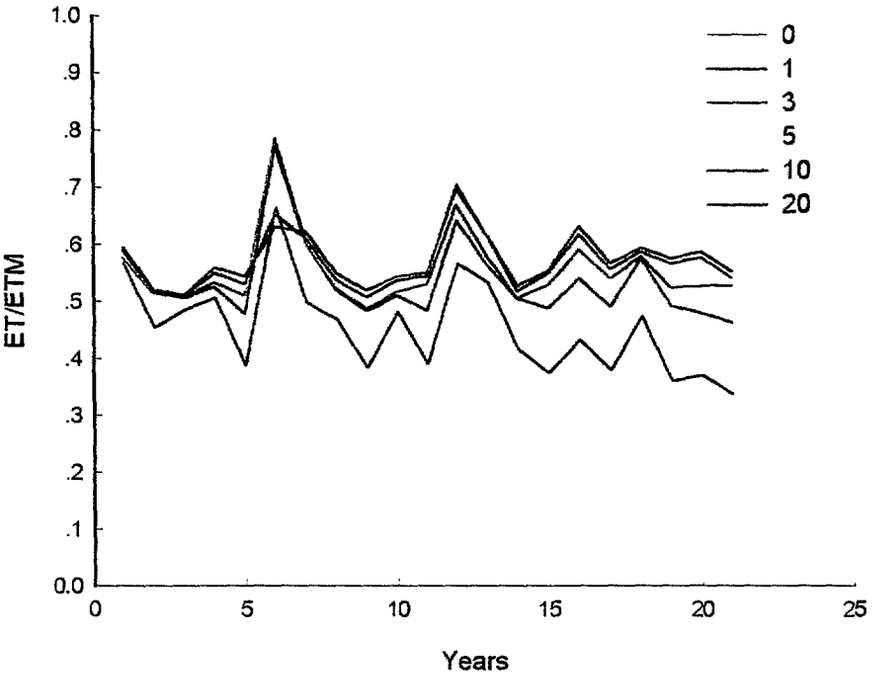

Figure 9. ET/Etma for a soil profile with a depth of 1m during the study period for different watershed surfaces (η).

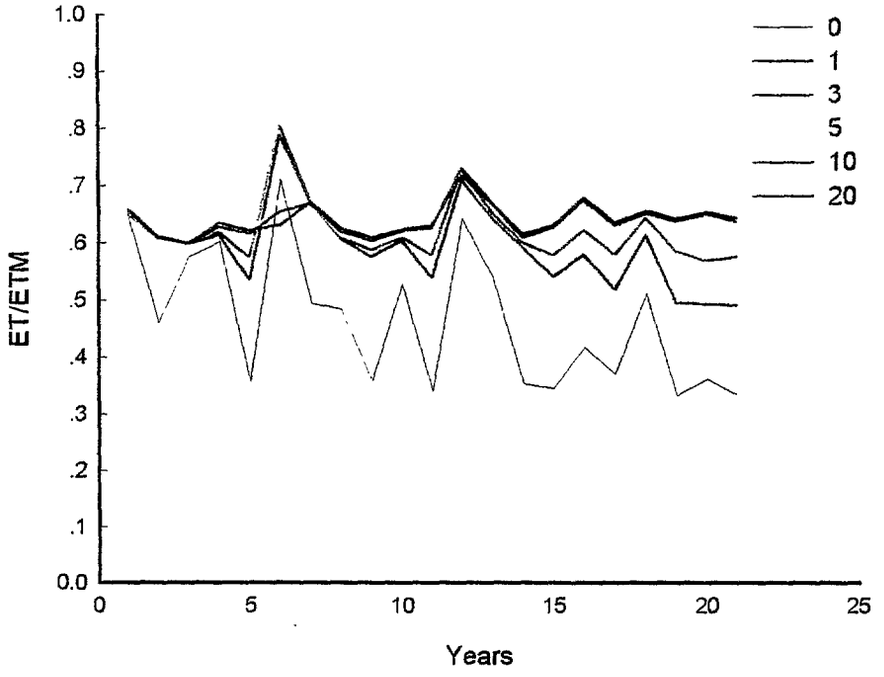

Figure 10. ET/ETma for a soil profile with a depth of 1.5m during the study period for different watershed surfaces (η).

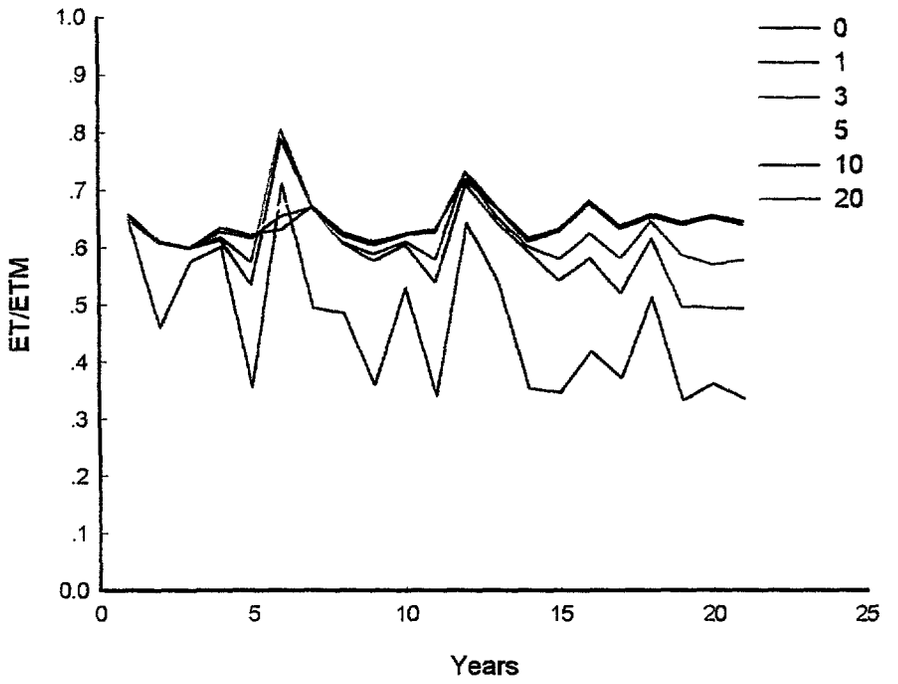

Figure 11. ET/ETM for a soil profile with a depth of 2m during the study period for different watershed surfaces (η).

The total amounts of water available in the soil profile (i.e. above wilting point) after harvest are presented in figures 12 to14 for 0.5, 1 and 2m of soil depth, respectively. Relatively large amounts were left in the soil profile for those years during which high amounts of summer rainfall were recorded.

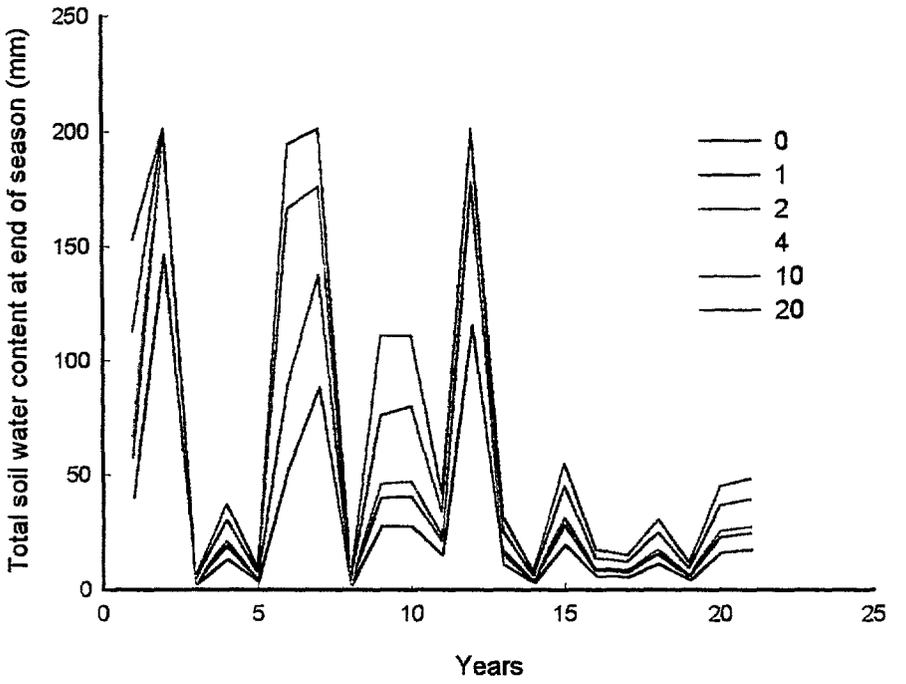

Figure 12. The total amount of water available in the soil profile (i.e. above wilting point) after harvest at a soil depth of 0.5m for different watershed surfaces (η).

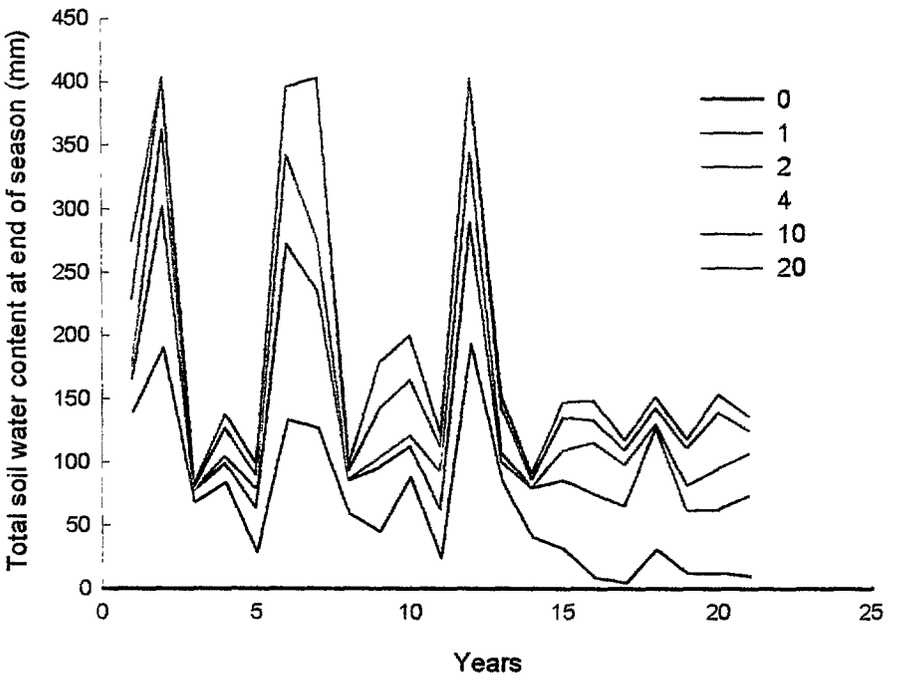

Figure 13. The total amount of water available in the soil profile (i.e. above wilting point) after harvest for a soil profile with a depth of 1.5m during the study period for different watershed surfaces (η).

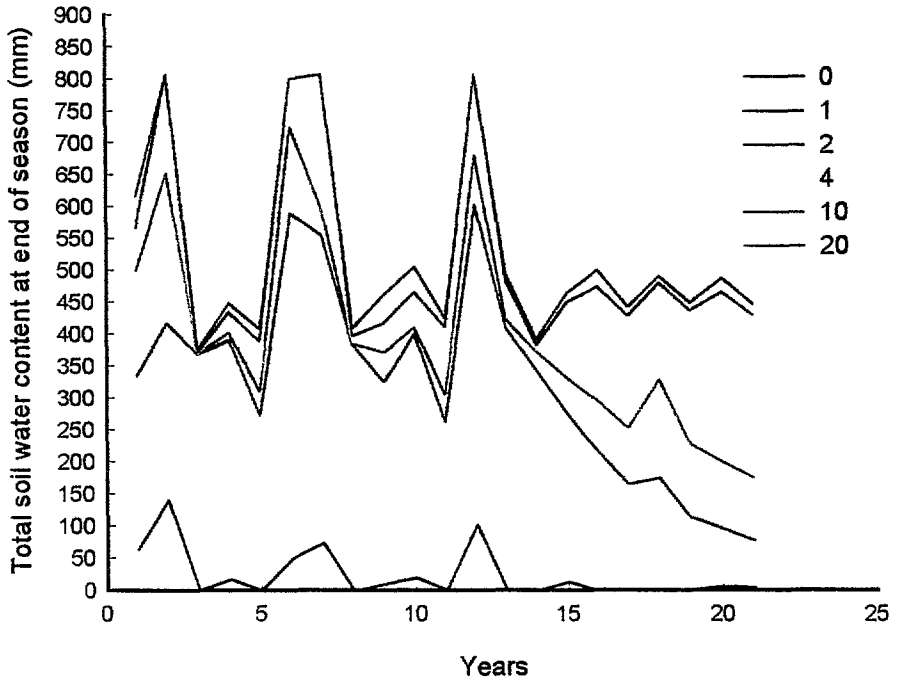

Figure 14. The total amount of water available in the soil profile (i.e. above wilting point) after harvest for a soil profile with a depth of 2m during the study period for different watershed surfaces (η).

In figure 15 the average evapotranspiration ratios are presented as a function of η. For the deeper profiles the curve flattens out for η between 3 and 4. For the shallowest soil profile there is an increase, albeit a small one, for all the ratios considered.

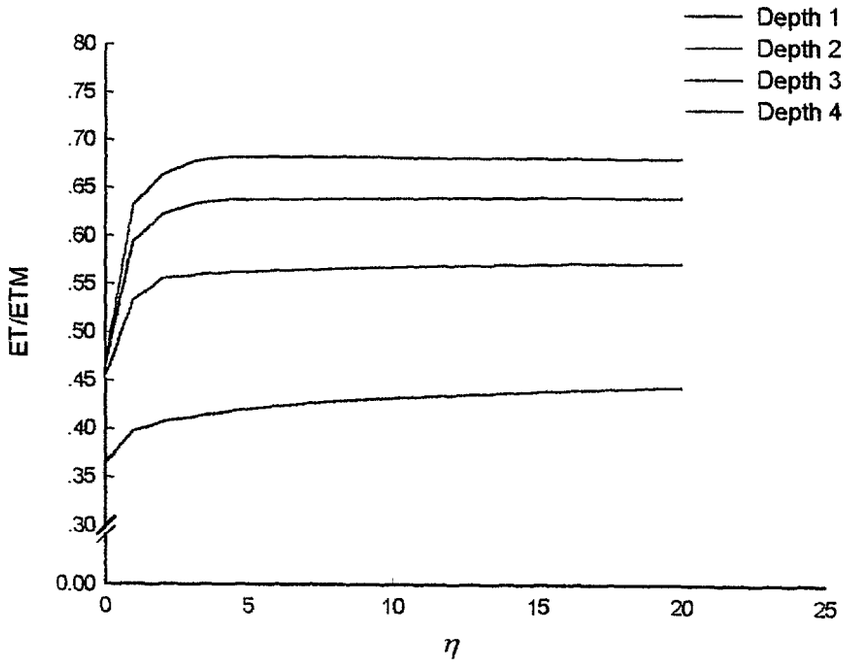

Figure 15. Relative increase in evapotranspiration ratio for different soil depths.

In figure 16 the increase in the average evapotranspiration ratio relative to the case with no runoff addition is presented. The highest increase (47 %) was observed for the deepest profile at η=4. In the shallower depths maximum value was not reached and an increase in η resulted in small gains.

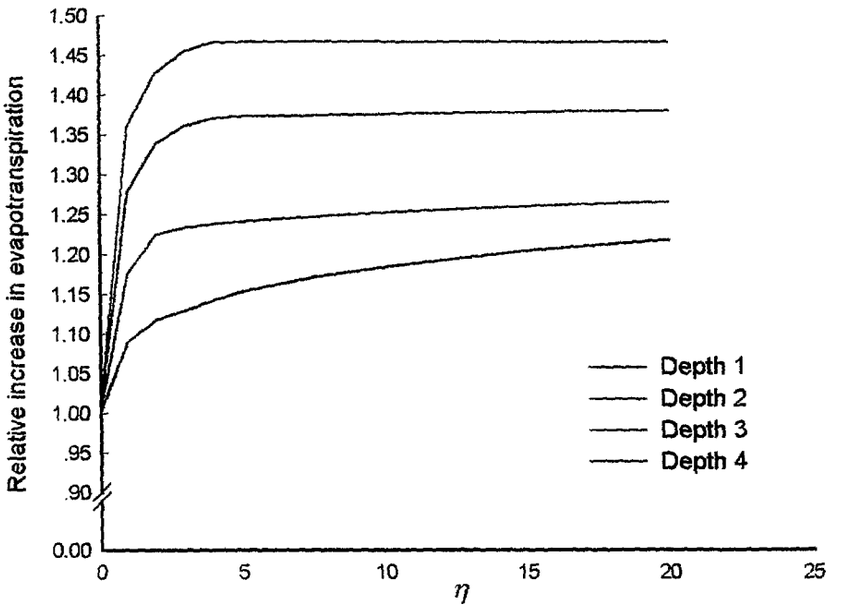

Figure 16. Relative increase in the average evapotranspiration ratio relative to the case with no runoff addition for different soil depths.

The effect of soil depth is presented in figure17 in which the ET ratio relative to the ET of the shallowest profile is presented. The maximum shifts to higher η's with an increase in soil depth.

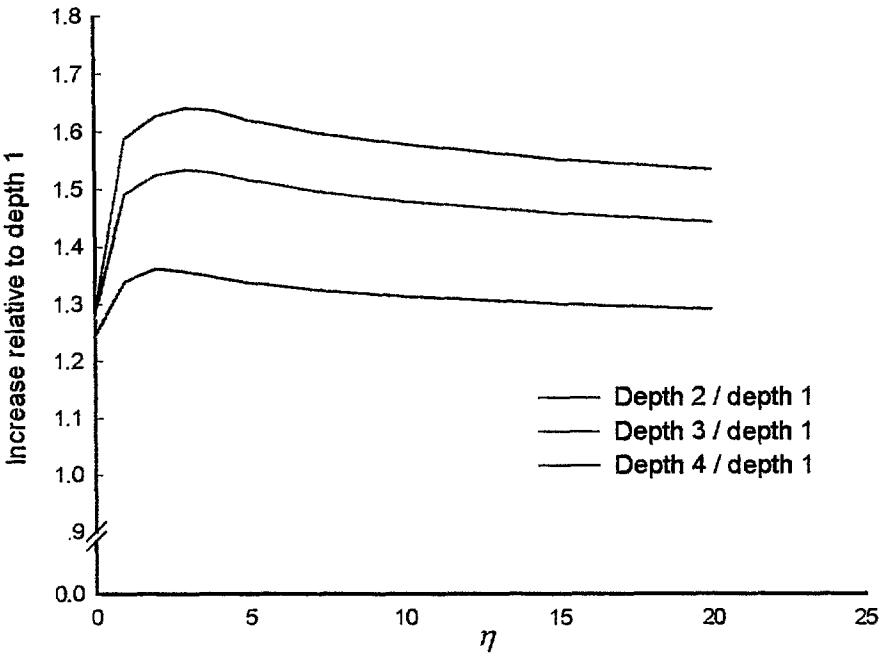

Figure 17. Evapotranspiration ratio relative to the evapotranspiration of the shallowest profile for different soil depths.

We defined the relative efficiency ratio (RE) as:

$$RE=\frac{Y_\eta}{Yo(1+\eta)}$$

Where Y_η and Y_o represent the yields obtained with and without the addition of runoff. In order to make the collection of runoff worthwhile the ratio has to be larger than one. RE>1 indicates that the addition of runoff from a given contributing area increases the yield in the receiving area by an amount that exceeds the production that would have been obtained on the contributing area (without the addition of runoff). The computed RE's for the period studied are presented for the extreme depths considered in this study in figures 18 and 19. The ratio decreases with an increase in η and is usually below 0.5. This indicates that according to our simulation there is no advantage in collecting runoff even during drier years.

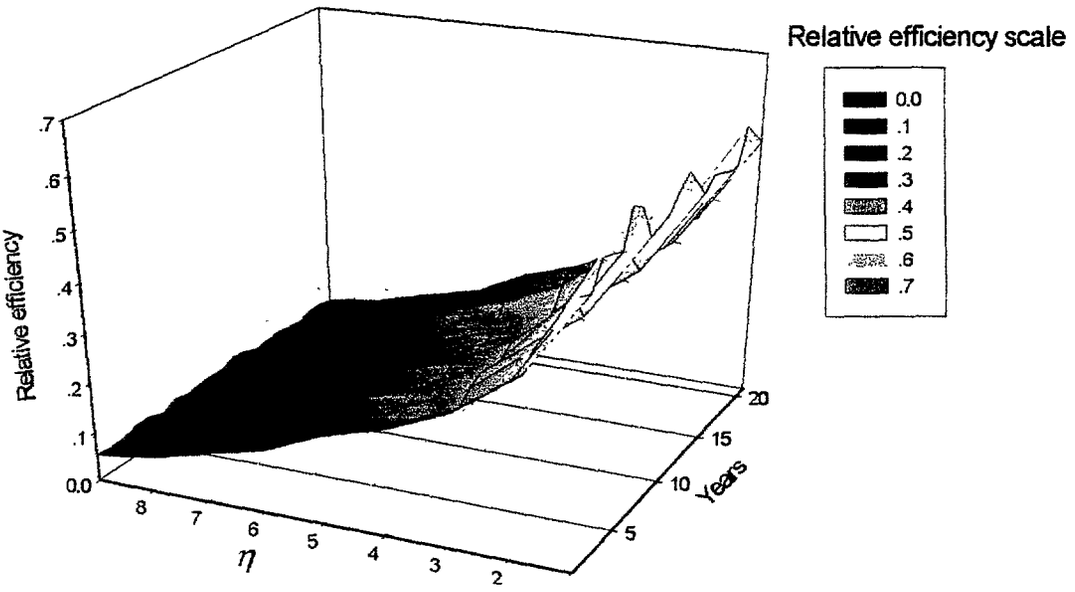

Figure 18. The relative efficiency for a soil depth of 0.5 m for different η's over the study period.

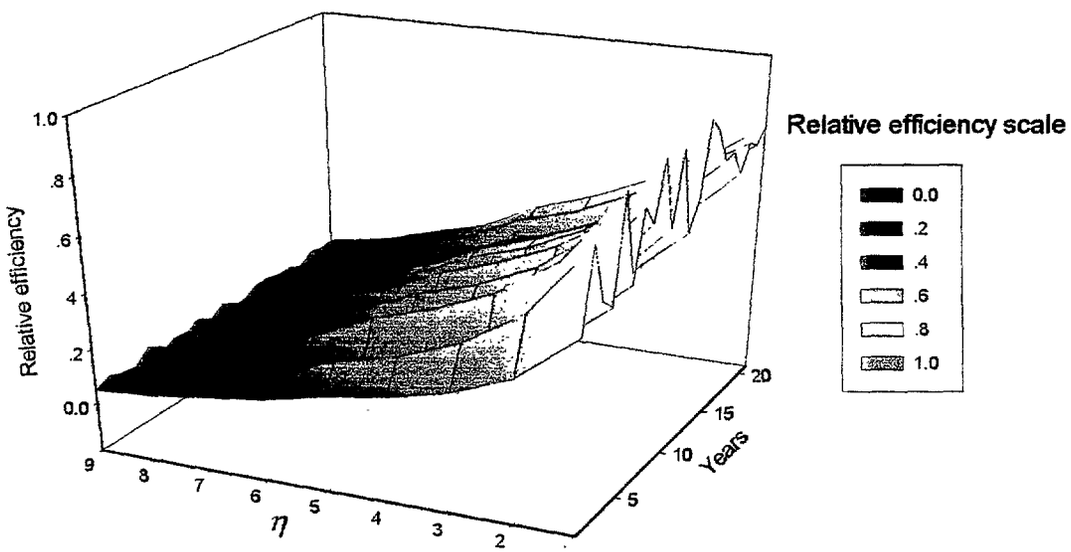

Figure 19. The relative efficiency for a soil depth of 4 m for different η's over the study period.

BIBLIOGRAPHY

Albergel, J. 1988. Genese et predetermination des crues au Burkina Faso. Collection Etudes et Theses, ORSTOM, Paris.

Amerman, C. and J. McGuinness. 1968. Plot and small watershed runoff: Its relation to larger areas. In: Trans. ASAE, 10(4), p. 464-466.

Brutsaert, W. 1982. Evaporation into the atmosphere. D. Reidel Publishing Company. Dordrecht, Holland.

Burgy, R., and C. Pomeroy. 1958. Interception losses in grassy vegetation. Transactions of the American Geophysical Union.

Dody, A., J. Ben-Asher, E. Adar. 1987. A parametric model for conversion of rainfall into runoff in small watershed in arid zones. A report. Ben-Gurion University of the Negev, 103pp.

Girard, G. 1975. Application du modele a discretisation spatiale au bassin versant de l'oued Ghorfa (Maurutanie), Cah. Orstom, Ser Hydrologie, Vol. 12, No 3, p. 167-188.

Hanks, R. J. 1992. Applied soil physics: soil, water and tempearture applications. Springer-Verlag. New York.

Harlin, J., and C. Kung, 1992. Parameter uncertainty and simulation of design floods in Sweden. J. Hydrology., 137: pp. 209-230.

Humborg, H. 1990. Ermittlung und Darstellung des Wasserertepotentials zur Bemessung von Sturzwasserbewasserungsanladen im Sahel unter Anwendung von Kenngroben aus Fernerkundungssystemen" unveroffentl. Diplomarbeit am Institut fur Wasserbau und Kulturtechnik, Universitat Karlsruhe, Karlsruhe.

Karnieli, A., J. Ben-Asher, A. Dody, A. Issar, G. Oron. 1988. An empirical approach for predicting runoff yield under desert conditions. Agric. Water manage., 14, p. 243-252.

Morris, E., and D. Woolhiser, 1980. Unsteady one-dimensional flow over a plane: Partial equilibrium and recession hydrographs. Water Resources Research 16(2): p. 355-360.

Osborn, H., and K. Renald 1973. Thunderstorm runoff on the Walnut Gulch experimental watershed, Arizona, USA, IAHS Publication No 97, p. 455-464.
Rawls, W., D. Brakensiek, K. Saxton. 1992. Estimation of soil water properties, Transactions of the American Society of Agricultural Engineers 25(5): 1316-1320, p.1328.

Renald, K.G. 1979. The hydrology of semi-arid rangeland watersheds. US Department of Agriculture, Agriculture Research Service, ARS 41-162, 25pp.

Schreiber, H., and D. Kincaid, 1967. Regression models for predicting on-site runoff from short durationconvective storms. Water Resources Research, Vol. 3, No 2, p. 389-395.

Sellers, W. D. 1965. Physical climatology. The University of Chicago. Chicago.

Tauer, M. and G. Humborg, 1992. Le potentiel d'irrigation par les eaux de ruissellement dans la region du Sahel. Institut fur Wasserbau und Kulturtechnik, Universitat Karlsruhe, Karlsruhe.

Woolhiser, D., and J. Liggett, 1967. Unsteady, one-dimensional flow over a plane – the rising hydrograph. Water Resources Research, 3 (3): pp. 753-771.

Woolhiser, D.A., R. Smith, and D. Goodrich. 1990. KINEROS, A Kinematic Runoff and Erosion Model: Documentation and User Manual. US Department of Agriculture, Agriculture Research Service, ARS 77, 130 pp.